British Journal of Cancer (2009) 101, 1549–1554

www.bjcancer.com

Clinical Studies

A phase-II trial of dose-dense chemotherapy in patients with disseminated thymoma: report of a Japan Clinical Oncology Group trial (JCOG 9605)

H Kunitoh*[,1,9], T Tamura[1], T Shibata[2], K Nakagawa[3], K Takeda[4], Y Nishiwaki[5], Y Osaki[6], K Noda[7], A Yokoyama[8], N Saijo[3,10] and JCOG Lung Cancer Study Group, Tokyo, Japan

[1]*Department of Medical Oncology, National Cancer Center Hospital, 5-1-1 Tsukiji, Chuo-ku, Tokyo 104-0045, Japan;* [2]*JCOG Data Center, Center for Cancer Control and Information Services, National Cancer Center, 5-1-1 Tsukiji, Chuo-ku, Tokyo 104-0045, Japan;* [3]*Department of Medical Oncology, Kinki University School of Medicine, 377-2 Ohnohigashi, Osakasayama, Osaka 589-8511, Japan;* [4]*Department of Medical Oncology, Osaka City General Hospital, 2-13-22 Miyakojima-Hondori, Miyakojima-ku, Osaka 534-0021, Japan;* [5]*Department of Thoracic Oncology, National Cancer Center Hospital East, 6-5-1 Kashiwanohara, Kashiwashi, Chiba 277-8577, Japan;* [6]*Department of Internal Medicine, Asahikawa Medical College, 1-1-1 Higashinijou, Midorigaoka, Asahikawa, Hokkaido 078-8510, Japan;* [7]*Division of Thoracic Oncology, Kanagawa Cancer Center, 1-1-2 Nakao, Asahi-ku, Yokohama, Kanagawa 241-0815, Japan;* [8]*Department of Medical Oncology, Niigata Cancer Center, 2-15-3, Kawagishi-cho, Niigata-shi, Niigata 951-8566, Japan;* [9]*Department of Respiratory Medicine, Mitsui Memorial Hospital, 1 Kandaizumicho, Chiyoda-ku, Tokyo 101-8643, Japan;* [10]*National Cancer Center Hospital East, 6-5-1 Kashiwanoha, Kashiwashi, Chiba 277-8577, Japan*

BACKGROUND: To evaluate the safety and efficacy of dose-dense weekly chemotherapy in the treatment of advanced thymoma.

METHODS: Subjects comprised patients with histologically documented chemotherapy-naïve thymoma with stage-IVa or IVb disease. Thymic carcinoma, carcinoid or lymphoma cases were excluded. Patients received 9 weeks of chemotherapy: cisplatin (25 mg m^{-2}) on weeks 1–9; vincristine (1 mg m^{-2}) on weeks 1, 2, 4, 6 and 8; and doxorubicin (40 mg m^{-2}) and etoposide (80 mg m^{-2}) on days 1–3 of weeks 1, 3, 5, 7 and 9. Chemotherapy courses were supported by granulocyte colony-stimulating factor. Post-protocol local therapy was allowed.

RESULTS: From July 1997 to March 2004, 30 patients were entered. Three were ineligible due to different histology. Chemotherapy-associated toxicity was mainly haematological and was well tolerated, with no deaths due to toxicity, and 87% of patients completed the planned 9-week regimen. Overall response rate was 59%, with 16 of the 27 eligible patients achieving partial response. Median progression-fee survival (PFS) was 0.79 years (95% confidence interval: 0.52–1.40 years), and PFS at 1 and 2 years was 37 and 15%, respectively. Overall survival rates at 2 and 5 years were 89 and 65%, respectively.

CONCLUSION: In stage-IV thymoma patients, weekly dose-dense chemotherapy offers similar activity to conventional regimens.

British Journal of Cancer (2009) **101**, 1549–1554. doi:10.1038/sj.bjc.6605347 www.bjcancer.com
Published online 6 October 2009

Keywords: thymoma; chemotherapy; dose-dense; platinum; anthracycline; granulocyte colony-stimulating factor

Thymoma is a rare thoracic tumour, but remains one of the most common tumours originating in the mediastinum (Thomas *et al*, 1999; Giaccone, 2005; Girard *et al*, 2009). Clinical behaviour tends to be indolent, but dissemination into the pleural space eventually occurs and sometimes distant metastasis arise (Thomas *et al*, 1999). Thymoma is frequently associated with paraneoplastic syndromes such as myasthenia gravis or pure red cell aplasia (Thomas *et al*, 1999; Giaccone, 2005). No International Union Against Cancer (UICC) TNM classification is available, and the Masaoka classification has been widely used for clinical staging (Masaoka *et al*, 1981; Girard *et al*, 2009).

*Correspondence: Dr H Kunitoh; E-mail: hkkunito@mitsuihosp.or.jp
Presented in part at the 42nd Annual Meeting of the American Society of Clinical Oncology, June 2-June 6, 2006, Atlanta, GA, USA
Received 3 June 2009; revised 4 September 2009; accepted 4 September 2009; published online 6 October 2009

The majority of thymomas are discovered at a limited stage, representing Masaoka stage-I or II, and surgical resection is the treatment of choice for such cases (Thomas *et al*, 1999; Giaccone, 2005; Girard *et al*, 2009). Even when the tumour invades neighbouring organs, as stage-III disease, surgical resection with postoperative radiotherapy is the preferred treatment when complete resection can be achieved (Curran *et al*, 1988; Urgesi *et al*, 1990; Ogawa *et al*, 2002; Strobel *et al*, 2004).

Systemic chemotherapy is usually used for stage-IVa (with pleural or pericardial dissemination) or stage-IVb disease (with lymphogenous or haematogenous metastases), but optimal management is less well established (Thomas *et al*, 1999; Girard *et al*, 2009). Several reports have described favourable outcomes in limited numbers of patients with stage-IVa disease treated using multimodal treatment including surgery (Kim *et al*, 2004; Yokoi *et al*, 2007).

Conversely, thymomas are generally reported to be chemotherapy-sensitive tumours, with response rates of 50–70% to

combination chemotherapy (Fornasiero *et al*, 1990; Loehrer *et al*, 1994, 1997, 2001; Giaccone *et al*, 1996; Berruti *et al*, 1999; Kim *et al*, 2004; Lucchi *et al*, 2006; Yokoi *et al*, 2007). Active agents include cisplatin (CDDP), vincristine (VCR), doxorubicin (ADM), etoposide (ETP), cyclophosphamide (CPM) and ifosfamide (IFX). Recent reports have shown marginal activity of pemetrexed (Loehrer *et al*, 2006) and combined carboplatin and paclitaxel (Lemma *et al*, 2008).

Dose-dense chemotherapy with the CODE combination (CDDP–VCR–ADM–ETP) and addition of granulocyte colony-stimulating factor (G-CSF) can be safely administered to patients with advanced lung cancer (Murray *et al*, 1991; Fukuoka *et al*, 1997). Theoretically, this approach might be suitable for chemosensitive tumours such as small-cell lung cancer and thymoma (Goldie and Coldman, 1983, 1984; Levin and Hryniuk, 1987; Murray, 1987). Because some pilot data in Japan suggested that administration of 12 weeks of the CODE chemotherapy was barely feasible, subsequent Japanese trials used a modified schedule, which was shortened to 9 weeks (Fukuoka *et al*, 1997; Furuse *et al*, 1998).

In 1996, the Japan Clinical Oncology Group (JCOG) initiated two clinical trials for advanced thymoma: one aimed at evaluating the safety and efficacy of the CODE regimen in stage IV, disseminated thymoma (JCOG 9605), and the other aimed at evaluating the safety and efficacy of CODE combination chemotherapy followed by surgical resection and postoperative radiotherapy in initially unresectable stage-III thymoma (JCOG 9606). The primary endpoint in each study was progression-free survival (PFS). The results of JCOG 9605 are reported herein.

PATIENTS AND METHODS

Eligibility criteria

Patients with chemotherapy-naive, histologically documented thymoma at Masaoka stage IVa or IVb were eligible for entry into the study. Thymoma must have been confirmed histologically and thymic tumours with other histology, such as thymic carcinoma, carcinoid or lymphoma, were excluded. Each patient was required to fulfil the following criteria: age, 15–70 years; Eastern Cooperative Oncology Group (ECOG) performance status (PS), 0–2; adequate organ function, that is, leukocyte count $\geqslant 4000\,\mu l^{-1}$, platelet count $\geqslant 10^5\,\mu l^{-1}$, hemoglobin $\geqslant 10.0\,g\,dl^{-1}$, serum creatinine <1.5 mg dl^{-1}, creatinine clearance $\geqslant 60\,ml\,min^{-1}$, serum bilirubin <1.5 mg dl^{-1}, serum alanine transaminase and aspartate transaminase levels less than double the upper limit of the institutional normal range; and $PaO_2 \geqslant 70$ mm Hg. Exclusion criteria included uncontrolled heart disease, uncontrolled diabetes or hypertension, pulmonary fibrosis or active pneumonitis as evidenced on chest radiography, infections necessitating systemic use of antibiotics, disease necessitating emergency radiotherapy such as superior vena cava obstruction syndrome, active concomitant malignancy and women who were pregnant or lactating. Also excluded were those patients with grave complications of thymoma, such as pure red cell aplasia or hypogammaglobulinemia. Myasthenia gravis was allowed and these patients were not excluded *per se*.

Patient eligibility was confirmed by the JCOG Data Center before patient registration. This study protocol was approved by the institutional review board at each participating centre and written informed consent was obtained from all patients prior to enrolment.

Treatment Plan

Chemotherapy Patients received the 9-week CODE combination chemotherapy as described below. Each chemotherapeutic agent was administered intravenously.

Week 1: CDDP 25 mg m^{-2} on day 1 with antiemetics and ample hydration; VCR (1 mg m^{-2}) on day 1; ADM (40 mg m^{-2}) on day 1 and ETP (80 mg m^{-2}) on days 1–3.

Weeks 2, 4, 6 and 8: CDDP (25 mg m^{-2}) on day 1 with antiemetics and ample hydration and VCR (1 mg m^{-2}) on day 1.

Weeks 3, 5, 7 and 9: CDDP (25 mg m^{-2}) on day 1 with antiemetics and ample hydration, ADM (40 mg m^{-2}) on day 1 and ETP (80 mg m^{-2}) on days 1–3.

Each week, G-CSF (filgrastim ($50\,\mu g\,m^{-2}\,day^{-1}$) or lenograstim ($2\,\mu g\,kg^{-1}\,day^{-1}$)) was administered by subcutaneous injection, except on days when chemotherapy was administered or when leukocyte count was $\geqslant 10\,000\,\mu l^{-1}$. Corticosteroid was used only as part of the antiemetic regimen, and the specific drug and dosage were not regulated by the protocol.

Dose and schedule modifications were performed as follows: when leukocyte count decreased to $<2{,}000\,\mu l^{-1}$ or platelet count decreased to $<50\,000\,\mu l^{-1}$, chemotherapy was delayed by 1 week. If PS decreased to 3–4 or temperature reached $\geqslant 38.0$°C, therapy was likewise delayed for 1 week. No dose modification of chemotherapy drugs was adopted for toxicity.

Post-protocol therapy

Surgery or radiotherapy was allowed after the completion of chemotherapy, at the discretion of the attending physician, even in the absence of apparent tumour regrowth. Conversely, additional chemotherapy without evidence of disease progression was not allowed.

Post-treatment after disease progression was not limited by the study protocol.

Patient evaluation and follow-up

Before enrolment into the study, each patient underwent complete medical history taking and physical examination (including neurological check-up for signs of myasthenia gravis), determination of blood cell counts, serum biochemistry testing, arterial blood gas analysis, pulmonary function testing, electrocardiography, chest radiography, computed tomography (CT) of the chest, CT or ultrasonography of the upper abdomen, whole-brain CT or magnetic resonance imaging (MRI) and an isotope bone scan. Blood-cell counts, serum biochemistry testing and chest radiography were performed weekly during each course of chemotherapy.

The toxicity of chemotherapy was evaluated according to the JCOG Toxicity Criteria (Tobinai *et al*, 1993), modified from version 1 of the National Cancer Institute Common Toxicity Criteria (NCI-CTC). Tumour responses were assessed radiographically according to the standard, two-dimensional WHO criteria (Miller *et al*, 1981), and were classified as complete response (CR), partial response (PR), no change (NC), progressive disease (PD) or non-evaluable (NE). After completion of the protocol therapy, patients were followed up with periodic re-evaluation, including chest CT every 6 months for the first 2 years and annually thereafter.

Central review

Radiographic reviews for the eligibility of enrolled patients and clinical responses were performed at the time of the study group meeting, held every 3–4 months. The study coordinator (H Kunitoh) and a few selected investigators from the group reviewed the radiographic films. The clinical response data presented below were all confirmed by this central review. Reviews of pathological specimens were not performed, because of insufficient logistics of the study group at the time of the study activation in 1997.

Endpoints and statistical considerations

The primary endpoint in each study was PFS. Due the rarity of the tumour and the accrual reported in US trials, which required 10 years to register 26 patients with locally advanced (stage-III) disease (Loehrer *et al*, 1997) and 9 years for 31 patients with disseminated (stage-IV) disease (Loehrer *et al*, 1994), we presumed we would be capable of accruing 30 patients in the target accrual period of 4 years. The sample size was, therefore, not determined based on statistical calculations. The expected PFS for the JCOG 9605 study was 2 years, which would give a 95% confidence interval of 1.3–3.0 years with 30 cases.

The initial study design thus envisioned enrolment of 30 fully eligible cases over 3 years for the study, with a follow-up period of 2 years.

Secondary endpoints included toxicity and safety, objective tumour response to chemotherapy, pattern of relapse, and overall survival (OS).

Progression-free survival and OS were calculated from the date of enrolment and estimated using the Kaplan–Meier method. Progression-free survival was censored at the last date verifiable as progression-free, and OS was censored as of the date of last follow-up. During the accrual period, an interim analysis for futility was planned after half of the patients had been registered and followed for $\geqslant 3$ months. All analyses were performed using SAS software version 8.2/9.1 (SAS Institute, Cary, NC, USA).

RESULTS

Patient characteristics

A total of 30 patients from seven institutions were enrolled from July 1997 to March 2004. Three patients were later found ineligible due to wrong histology, with two cases of thymic carcinoma and one case of carcinoid. These mistakes occurred due to technical problems in the patient registry. Since the ineligible cases did receive the protocol therapy, all 30 patients were analysed for characteristics and toxicity. Twenty-seven eligible patients were analysed for clinical response and survival (PFS and OS). Patient characteristics are shown in Table 1.

Table 1 Patient characteristics

Item	
Sex	
Male/female	16/14
Age (years)	
Median/range	47.5/29–69
ECOG performance status	
PS0/PS1/PS2	11/18/1
Masaoka stage	
IVa/IVb	22/8
Smoking history	
No	9
Yes (median pack–years)	21 (22)
Myasthenia gravis	
No/yes	28/2
Histology: thymoma and eligible	27
Lymphocyte predominance	12
Mixed cell	9
Epithelioid cell	4
Clear cell	1
Spindle cell	0
Unclassified	1
Histology: not thymoma (ineligible)	3
Carcinoma	2
Carcinoid	1
Lymphoma	0
Prior therapy	
None	26
Surgery	2
Surgery and radiation	2

Abbreviations: ECOG = Eastern Cooperative Oncology Group; PS = performance status.

Chemotherapy delivery and toxicity

Nine weeks of chemotherapy were performed for 26 of the original 30 patients (87%). The other four patients included one patient receiving 7 weeks, two receiving 6 weeks and one receiving 3 weeks of therapy. Median duration of chemotherapy for the 26 patients who underwent the planned nine cycles was 10 weeks (range, 9–12 weeks).

Table 2 summarises the major toxicities of chemotherapy, which were mainly haematological. Although 70% of patients experienced grade-IV neutropenia, this was generally transient and rarely complicated by infection/fever. Overall, toxicities were well tolerated and no deaths due to toxicity occurred.

Table 2 Toxicity of chemotherapy ($n = 30$)

Toxicity	Grades 1/2	Grade 3	Grade 4	%Grade 3/4
Leukopenia	3/6	12	8	67
Neutropenia	3/1	5	21	87
Anemia	0/5	25	ND	83
Thrombocytopenia	4/6	5	3	27
ALT	9/0	0	0	0
Creatinine	2/1	0	0	0
PaO_2	9/2	0	0	0
Emesis	13/11	2	ND	7
Diarrhoea	4/2	0	0	0
Stomatitis	4/3	0	0	0
Constipation	3/4	2	0	7
Neuropathy	11/2	0	ND	0
Infection	3/4	3	0	10

Abbreviations: ALT = alanine transaminase; ND = not defined (the JCOG toxicity criteria did not define grade IV in these toxicities).

Other and late complications

Four patients showed thymoma-related complications. One patient suffered from myasthenia gravis crisis occurring during chemotherapy, but subsequently recovered. Another patient showed newly diagnosed myasthenia gravis 2.5 years after completion of the protocol therapy, and thymectomy and resection of the residual tumour were performed. Two other cases had pure red cell aplasia occurring later in the clinical course with disease progression of the thymomas.

Clinical response to chemotherapy

Clinical responses of the 27 eligible patients to chemotherapy were judged radiologically and confirmed by central review. Responses were as follows: CR, 0 patients; PR, 16 patients; NC, 10 patients and PD, 1 patient. Overall response rate was 59% (95% confidence interval, 39–78%).

Post-protocol therapy

Post-protocol local therapy was administered to 18 of the 27 eligible patients (67%). Eight patients (all with stage-IVa disease) underwent surgical resection and 13 patients (nine with stage-IVa disease and four with stage-IVb disease) received thoracic radiotherapy, with three patients receiving both. Whether patients received local therapy after disease progression was not recorded on case report forms.

After disease progression, 16 of the 27 patients (59%) received additional chemotherapy. Post-protocol chemotherapy included platinum re-challenge, irinotecan, taxanes and investigational agents. Clinical response data to those therapies are not available.

PFS and OS

Survival data were finally updated in March 2006, 2 years after accrual of the last patient. Figure 1 shows PFS and OS curves of the 27 eligible patients. Median PFS was 0.79 years (95% confidence interval, 0.52–1.40 years) and PFS at 1 and 2 years was 37 and 15%, respectively. Median OS was 6.1 years and OS at 2 and 5 years was 89 and 65%, respectively.

Overall survival was longer for stage-IVa patients than for stage-IVb patients (Figure 2, median, 6.8 years and 3.5 years, respectively), but PFS was similar (Figure 3, median, 0.79 years for IVa patients and 0.78 years for IVb patients).

Pattern of relapse

As of the data cut-off, 26 of the 27 eligible patients had experienced tumour relapse. Sites of initial relapse comprised the primary site only in seven cases (27%), pleural or pericardial dissemination in seven cases (27%) and primary site and pleural/pericardial dissemination in nine cases (35%). Thus, 23 of the 26 patients with relapse initially showed regrowth of the primary and/or pleural or pericardial dissemination, with only three patients (12%) showing initial relapse at distant organs.

DISCUSSION

Few prospective trials of chemotherapy have been described for patients with advanced thymoma. Most prior studies have combined stage-III, localised disease and stage-IV, disseminated disease (Table 3). In addition, most have also included both thymoma and thymic carcinoma histology.

We have reported results for patients with stage-IV disease, for which systemic therapy should be the first choice. Among previous studies, only those from the ECOG separately reported results for stage-III and stage-IV patients (Loehrer *et al*, 1994, 1997). The ECOG took 9 years to accrue 31 patients with stage-IV disease, including patients with thymic carcinoma (Loehrer *et al*, 1994). We prospectively accrued patients with thymoma only and excluded thymic carcinoma, as thymoma and thymic carcinoma clearly differ in clinical presentation and prognosis, and trials involving these pathologies should, thus, be reported separately (Eng *et al*, 2004; Giaccone, 2005; Lemma *et al*, 2008).

Trials of systemic chemotherapy for thymoma have reported response rates of 50–90%, so this tumour is generally considered sensitive to chemotherapy (Thomas *et al*, 1999). Dose-dense chemotherapy such as the CODE four-drug combination has been argued to be theoretically suitable for the treatment of such chemosensitive tumours (Murray, 1987).

Although our results showed that dose-dense CODE chemotherapy could be safely administered to thymoma patients, efficacy was not remarkable. The overall response rate was about 60%, no different from prior reports employing conventional-dose chemotherapy (Table 3). Progression-free survival was 9 months, falling far short of the expected 2 years. Although OS studies compared favourably with the corresponding ECOG trial (Loehrer *et al*, 1994), attempting to reach a valid conclusion would be difficult due to the small sample sizes. In addition, OS could be

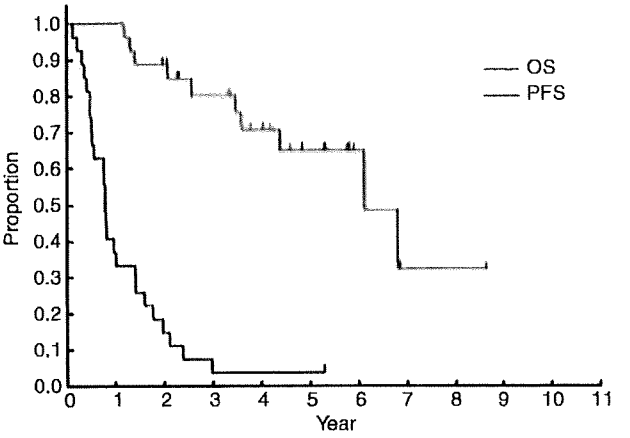

Figure 1 Progression-free survival and OS of the 27 eligible patients.

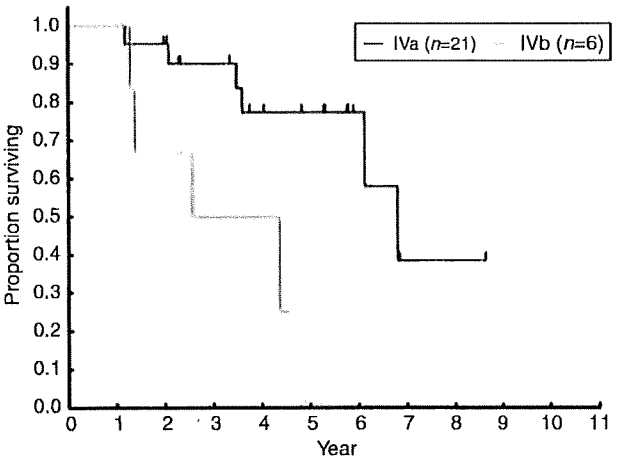

Figure 2 Overall survival according to Masaoka stage (stage IVa *vs* IVb).

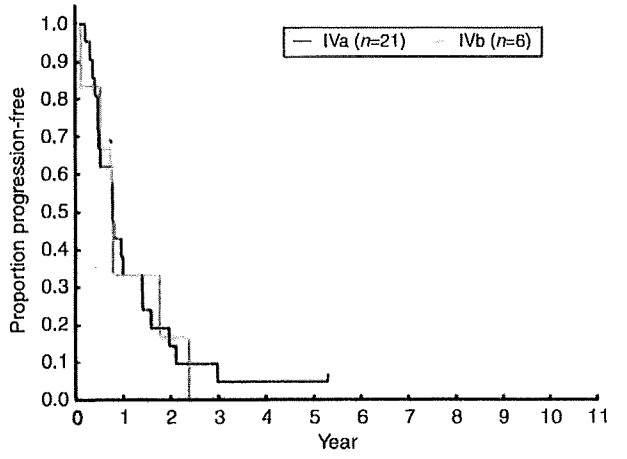

Figure 3 Progression-free survival according to Masaoka stage (stage IVa *vs* IVb).

Table 3 Reports of combination chemotherapy for thymoma

Regimen	Stage	Patients[a]	ORR	Reference
Anthracycline-containing regimens				
ADOC (S)	III/IV	32	91%	Fornasiero *et al* (1990)
PAC (G)	IV	30	50%	Loehrer *et al* (1994)
PAC (G)	III	23	70%	Loehrer *et al* (1997)
ADOC (S)	III/IV	16	81%	Berruti *et al* (1999)
PAC (G)	III/IV	22	77%	Kim *et al* (2004)
PAE (S)	III/IV	30	73%	Lucchi *et al* (2006)
CAMP (S)	III/IV	14	93%	Yokoi *et al* (2007)
CODE (G)	IV	27	59%	Current study
Non-anthracycline-containing regimens				
PE (G)	III/IV	16	56%	Giaccone *et al* (1996)
VIP (G)	III/IV	20	35%	Loehrer *et al* (1997)
CP (G)	III/IV	23	35%	Lemma *et al* (2008)

Abbreviations: ADOC = doxorubicin, cisplatin, vincristine, cyclophosphamide; CAMP = cisplatin, doxorubicin, methylpredonisolone; CODE = cisplatin, vincristine, doxorubicin, etoposide; CP = carboplatin, paclitaxel; G = prospective multicenter group trial; ORR = overall response rate; PAC = cisplatin, doxorubicin, cyclophosphamide; PAE = cisplatin, epidoxorubicin, etoposide; PE = cisplatin, etoposide; S = single-center experience; VIP = etoposide, ifosfamide, cisplatin. [a]Number of assessable patients.

greatly affected by post-study local therapy especially in patients with stage-IVa disease, as combined therapy trial including stage-IVa patients suggested (Kim *et al*, 2004). In fact, this might be one reason why OS of stage-IVa patients was much longer than that of stage-IVb patients, whereas PFS was similar.

It could be argued that shortened CODE chemotherapy, used in Japan due to feasibility problem, led to inadequate results due to insufficient total dosages of chemotherapy drugs. However, another intensive chemotherapy, ETP–IFX–CDDP (VIP) supported by G-CSF, has also reported disappointingly low response rates and no better survival (Loehrer *et al*, 2001). Hanna *et al* (2001) reported five patients with prior chemotherapy treated with high-dose chemotherapy and stem cell support, but concluded that no superiority to conventional therapy was evident. Taken together with our results, intensification of chemotherapy does not appear sufficiently promising for treating advanced thymoma.

Many prior chemotherapy studies have included platinum and anthracyclines in their regimens. Non-anthracycline approaches contained regimens such as VIP (Loehrer *et al*, 2001), ETP–CDDP (Giaccone *et al*, 1996) and paclitaxel–carboplatin (Lemma *et al*, 2008) tended to yield lower response rates of 32–56% as compared with regimens including anthracycline (Table 3). It might, thus, be suggested that both anthracycline and platinum should, thus, be included in thymoma chemotherapy, at least in current clinical practice.

Favourable results have recently been reported with multimodality therapy, including surgical resection of stage-IVa disease (Kim *et al*, 2004; Yokoi *et al*, 2007). In fact, about two-thirds of eligible patients in our trial received local therapy after chemotherapy, including surgery in eight patients. This could have affected the outcome of the patients, as discussed above. However, small sample size and patient selection preclude reaching any definitive conclusion. When and what local therapy, if any, would benefit patients with disseminated thymoma, remains yet to be established. Further studies are warranted.

The present study shows several additional limitations. One is that we did not perform a central review of histology, and, thus, could not provide WHO classifications of histology (Okumura *et al*, 2002; Travis *et al*, 2004). This makes comparisons with results from other reports difficult. Central pathology review and preferably tissue collection would be very important in future trials.

In addition, due to the shorter-than-expected PFS, the planned CT scan interval of every 6 months might not have accurately evaluated PFS (Freidlin *et al*, 2007). Future trials might require more frequent scans.

In conclusion, we have reported that weekly dose-dense chemotherapy can be safely administered to patients with thymoma. However, efficacy seems similar to that in patients treated with conventional doses. More research on optimal systemic therapy and the role of local modalities would appear to be necessary.

ACKNOWLEDGEMENTS

This work was supported by Grants-in-Aid for Cancer Research from the Ministry of Health, Labour and Welfare of Japan (11S-2, 11S-4, 14S-2, 14S-4, 17S-2, 17S-5).

REFERENCES

Berruti A, Borasio P, Gerbino A, Gorzegno G, Moschini T, Tampellini M, Ardissone F, Brizzi MP, Dolcetti A, Dogliotti L (1999) Primary chemotherapy with adriamycin, cisplatin, vincristine and cyclophosphamide in locally advanced thymomas: a single institution experience. *Br J Cancer* **81**: 841–845

Curran Jr WJ, Kornstein MJ, Brooks JJ, Turrisi 3rd AT (1988) Invasive thymoma: the role of mediastinal irradiation following complete or incomplete surgical resection. *J Clin Oncol* **6**: 1722–1727

Eng TY, Fuller CD, Jagirdar J, Bains Y, Thomas Jr CR (2004) Thymic carcinoma: state of the art review. *Int J Radiat Oncol Biol Phys* **59**: 654–664

Fornasiero A, Daniele O, Ghiotto C, Sartori F, Rea F, Piazza M, Fiore-Donati L, Morandi P, Aversa SM, Paccagnella A, Pappagallo GL, Fiorentino MV (1990) Chemotherapy of invasive thymoma. *J Clin Oncol* **8**: 1419–1423

Freidlin B, Korn EL, Hunsberger S, Gray R, Saxman S, Zujewski JA (2007) Proposal for the use of progression-free survival in unblinded randomized trials. *J Clin Oncol* **25**: 2122–2126

Fukuoka M, Masuda N, Negoro S, Matsui K, Yana T, Kudoh S, Kusunoki Y, Takada M, Kawahara M, Ogawara M, Kodama N, Kubota K, Furuse K (1997) CODE chemotherapy with and without granulocyte colony-stimulating factor in small-cell lung cancer. *Br J Cancer* **75**: 306–309

Furuse K, Fukuoka M, Nishiwaki Y, Kurita Y, Watanabe K, Noda K, Ariyoshi Y, Tamura T, Saijo N (1998) Phase III study of intensive weekly chemotherapy with recombinant human granulocyte colony-stimulating factor versus standard chemotherapy in extensive-disease small-cell lung cancer. *J Clin Oncol* **16**: 2126–2132

Giaccone G (2005) Treatment of malignant thymoma. *Curr Opin Oncol* **17**: 140–146

Giaccone G, Ardizzoni A, Kirkpatrick A, Clerico M, Sahmoud T, van Zandwijk N (1996) Cisplatin and etoposide combination chemotherapy for locally advanced or metastatic thymoma. A phase II study of the European Organization for Research and Treatment of Cancer Lung Cancer Cooperative Group. *J Clin Oncol* **14**: 814–820

Girard N, Mornex F, Van Houtte P, Cordier JF, van Schil P (2009) Thymoma: a focus on current therapeutic management. *J Thorac Oncol* **4**: 119–126

Goldie JH, Coldman AJ (1983) Quantitative model for multiple levels of drug resistance in clinical tumors. *Cancer Treat Rep* **67**: 923–931

Goldie JH, Coldman AJ (1984) The genetic origin of drug resistance in neoplasms: implications for systemic therapy. *Cancer Res* **44**: 3643–3653

Hanna N, Gharpure VS, Abonour R, Cornetta K, Loehrer Sr PJ (2001) High-dose carboplatin with etoposide in patients with recurrent thymoma: the Indiana University experience. *Bone Marrow Transplant* **28**: 435–438

Kim ES, Putnam JB, Komaki R, Walsh GL, Ro JY, Shin HJ, Truong M, Moon H, Swisher SG, Fossella FV, Khuri FR, Hong WK, Shin DM (2004) Phase II study of a multidisciplinary approach with induction chemotherapy, followed by surgical resection, radiation therapy, and consolidation chemotherapy for unresectable malignant thymomas: final report. *Lung Cancer* **44:** 369–379

Lemma GL, Loehrer Sr PJ, Lee JW, Langer CJ, Tester WJ, Johnson DH (2008) A phase II study of carboplatin plus paclitaxel in advanced thymoma or thymic carcinoma: E1C99. *J Clin Oncol* **26**(15S): abstract 8018

Levin L, Hryniuk WM (1987) Dose intensity analysis of chemotherapy regimens in ovarian carcinoma. *J Clin Oncol* **5:** 756–767

Loehrer Sr PJ, Chen M, Kim K, Aisner SC, Einhorn LH, Livingston R, Johnson D (1997) Cisplatin, doxorubicin, and cyclophosphamide plus thoracic radiation therapy for limited-stage unresectable thymoma: an intergroup trial. *J Clin Oncol* **15:** 3093–3099

Loehrer Sr PJ, Jiroutek M, Aisner S, Aisner J, Green M, Thomas Jr CR, Livingston R, Johnson DH (2001) Combined etoposide, ifosfamide, and cisplatin in the treatment of patients with advanced thymoma and thymic carcinoma: an intergroup trial. *Cancer* **91:** 2010–2015

Loehrer Sr PJ, Kim K, Aisner SC, Livingston R, Einhorn LH, Johnson D, Blum R (1994) Cisplatin plus doxorubicin plus cyclophosphamide in metastatic or recurrent thymoma: final results of an intergroup trial. The Eastern Cooperative Oncology Group, Southwest Oncology Group, and Southeastern Cancer Study Group. *J Clin Oncol* **12:** 1164–1168

Loehrer Sr PJ, Yiannoutsos CT, Dropcho S, Burns M, Helft P, Chiorean EG, Nelson RP (2006) A phase II trial of pemetrexed in patients with recurrent thymoma or thymic carcinoma. *J Clin Oncol* **24**(18S): abstract 7079

Lucchi M, Melfi F, Dini P, Basolo F, Viti A, Givigliano F, Angeletti CA, Mussi A (2006) Neoadjuvant chemotherapy for stage III and IVA thymomas: a single-institution experience with a long follow-up. *J Thorac Oncol* **1:** 308–313

Masaoka A, Monden Y, Nakahara K, Tanioka T (1981) Follow-up study of thymomas with special reference to their clinical stages. *Cancer* **48:** 2485–2492

Miller AB, Hoogstraten B, Staquet M, Winkler A (1981) Reporting results of cancer treatment. *Cancer* **47:** 207–214

Murray N (1987) The importance of dose and dose intensity in lung cancer chemotherapy. *Semin Oncol* **14:** 20–28

Murray N, Shah A, Osoba D, Page R, Karsai H, Grafton C, Goddard K, Fairey R, Voss N (1991) Intensive weekly chemotherapy for the treatment of extensive-stage small-cell lung cancer. *J Clin Oncol* **9:** 1632–1638

Ogawa K, Uno T, Toita T, Onishi H, Yoshida H, Kakinohana Y, Adachi G, Itami J, Ito H, Murayama S (2002) Postoperative radiotherapy for patients with completely resected thymoma: a multi-institutional, retrospective review of 103 patients. *Cancer* **94:** 1405–1413

Okumura M, Ohta M, Tateyama H, Nakagawa K, Matsumura A, Maeda H, Tada H, Eimoto T, Matsuda H, Masaoka A (2002) The World Health Organization histologic classification system reflects the oncologic behavior of thymoma: a clinical study of 273 patients. *Cancer* **94:** 624–632

Strobel P, Bauer A, Puppe B, Kraushaar T, Krein A, Toyka K, Gold R, Semik M, Kiefer R, Nix W, Schalke B, Muller-Hermelink HK, Marx A (2004) Tumor recurrence and survival in patients treated for thymomas and thymic squamous cell carcinomas: a retrospective analysis. *J Clin Oncol* **22:** 1501–1509

Thomas CR, Wright CD, Loehrer PJ (1999) Thymoma: state of the art. *J Clin Oncol* **17:** 2280–2289

Tobinai K, Kohno A, Shimada Y, Watanabe T, Tamura T, Takeyama K, Narabayashi M, Fukutomi T, Kondo H, Shimoyama M, Suemasu K (1993) Toxicity grading criteria of the Japan Clinical Oncology Group. The Clinical Trial Review Committee of the Japan Clinical Oncology Group. *Jpn J Clin Oncol* **23:** 250–257

Travis WB, Brambilla E, Muller-Hermelinck HK, Harris CC (2004) *Pathology and Genetics of Tumours of the Lung, Pleura, Thymus and Heart.* IARC Press: Lyon

Urgesi A, Monetti U, Rossi G, Ricardi U, Casadio C (1990) Role of radiation therapy in locally advanced thymoma. *Radiother Oncol* **19:** 273–280

Yokoi K, Matsuguma H, Nakahara R, Kondo T, Kamiyama Y, Mori K, Miyazawa N (2007) Multidisciplinary treatment for advanced invasive thymoma with cisplatin, doxorubicin, and methylprednisolone. *J Thorac Oncol* **2:** 73–78

Appendix 1

STUDY PARTICIPANTS

The following institutions and investigators participated in the trial:

Asahikawa Medical College (Yoshinobu Osaki), National Cancer Center Hospital East (Yutaka Nishiwaki, Kaoru Kubota, Nagahiro Saijo), National Cancer Center Hospital (Tomohide Tamura, Noboru Yamamoto, Hideo Kunitoh), Kanagawa Cancer Center (Kazumasa Noda, Fumihiro Oshita), Niigata Cancer Center Hospital (Akira Yokoyama, Yuko Tsukada), Kinki University Hospital (Kazuhiko Nakagawa, Isamu Okamoto) and Osaka City General Hospital (Koji Takeda, Haruko Daga).

Appendix 2

ACKNOWLEDGEMENTS

We thank Ms Mieko Imai for data management at the JCOG Data Center.

Published Online First on June 2, 2009 as 10.1158/0008-5472.CAN-08-4882

N-myc Downstream Regulated Gene 1/Cap43 Suppresses Tumor Growth and Angiogenesis of Pancreatic Cancer through Attenuation of Inhibitor of κB Kinase β Expression

Fumihito Hosoi,[1,3] Hiroto Izumi,[6] Akihiko Kawahara,[3,4] Yuichi Murakami,[1] Hisafumi Kinoshita,[5] Masayoshi Kage,[3,4] Kazuto Nishio,[7] Kimitoshi Kohno,[6] Michihiko Kuwano,[2] and Mayumi Ono[1]

[1]Department of Pharmaceutical Oncology, Graduate School of Pharmaceutical Sciences and [2]Innovation Center for Medical Redox Navigation, Kyushu University, Fukuoka, Japan; [3]Research Center for Innovative Cancer Therapy, Kurume University; [4]Department of Pathology, Kurume University Hospital; [5]Department of Surgery, Kurume University School of Medicine, Kurume, Japan; [6]Department of Molecular Biology, University of Occupational and Environmental Health, Kitakyushu, Japan; and [7]Department of Genome Biology, Kinki University School of Medicine, Osaka, Japan

Abstract

N-myc downstream regulated gene 1 (NDRG1)/Cap43 expression is a predictive marker of good prognosis in patients with pancreatic cancer as we reported previously. In this study, NDRG1/Cap43 decreased the expression of various chemoattractants, including CXC chemokines for inflammatory cells, and the recruitment of macrophages and neutrophils with suppression of both angiogenesis and growth in mouse xenograft models. We further found that NDRG1/Cap43 induced nuclear factor-κB (NF-κB) signaling attenuation through marked decreases in inhibitor of κB kinase (IKK) β expression and IκBα phosphorylation. Decreased IKKβ expression in cells overexpressing NDRG1/Cap43 resulted in reduction of both nuclear translocation of p65 and p50 and their binding to the NF-κB motif. The introduction of an exogenous IKKβ gene restored NDRG1/Cap43-suppressed expression of melanoma growth-stimulating activity α/CXCL1, epithelial-derived neutrophil activating protein-78/CXCL5, interleukin-8/CXCL8 and vascular endothelial growth factor-A, accompanied by increased phosphorylation of IκBα in NDRG1/Cap43-expressing cells. In patients with pancreatic cancer, NDRG1/Cap43 expression levels were also inversely correlated with the number of infiltrating macrophages in the tumor stroma. This study suggests a novel mechanism by which NDRG1/Cap43 modulates tumor angiogenesis/growth and infiltration of macrophages/neutrophils through attenuation of NF-κB signaling. [Cancer Res 2009;69(12):4983–91]

Introduction

N-myc downstream regulated gene 1 (NDRG1)/Cap43 is one of the metastasis suppressor genes (1), and expression of NDRG1/Cap43 is regulated by oncogenes (*N-myc* and *C-myc*) and tumor suppressor genes (*p53, VHL,* and *PTEN*; ref. 2). Expression of NDRG1/Cap43 protein is often elevated in many types of human tumors. In human cancer, expression of NDRG1/Cap43 depends on tumor type and differentiation status (2). Consistent with this idea, NDRG1/Cap43 expression in cancer cells is a predictive marker of good prognosis in patients with neuroblastoma or cancers of the prostate, breast, esophagus, colon, and pancreas (3–10), whereas its expression is a predictive marker of poor prognosis in patients with liver and cervical cancer (11, 12).

We previously identified *NDRG1/Cap43* as one of the nine genes that are highly expressed in cancerous regions of human renal cell carcinoma (13), and its expression is closely associated with the *VHL* oncosuppressor gene (14). We further showed that expression of NDRG1/Cap43 is associated with a marked decrease of tumor angiogenesis in mice bearing human pancreatic cancer xenografts and that NDRG1/Cap43 markedly suppresses the expression of matrix metalloproteinase-9, vascular endothelial growth factor (VEGF), and interleukin (IL)-8/CXCL8. Moreover, expression of NDRG1/Cap43 has been associated with decreased microvessel density (MVD) and differentiation or depth of invasion in cancer cells in patients with pancreatic cancer (5).

In the present study, we further examined how NDRG1/Cap43 modulates tumor growth and angiogenesis in pancreatic cancer. Because microarray analysis in this study and our previous studies showed that expression of some angiogenesis- and inflammation-related factors were markedly down-regulated by NDRG1/Cap43, we hypothesized that inflammation could be somehow associated with the NDRG1/Cap43-induced suppression of tumor growth and angiogenesis. Our results indicated that down-regulation of CXC chemokines and VEGF expression by NDRG1/Cap43 was actively involved in its suppression of angiogenesis and growth in pancreatic cancer as well as infiltration of macrophages and neutrophils, and we discuss whether attenuation of nuclear factor-κB (NF-κB) signaling plays a key role in this process.

Materials and Methods

Materials and cell lines. MIApaca-2 transfectants (Mock#2, Cap#11 and Cap#14) were maintained in DMEM supplemented with 10% fetal bovine serum and G418. The anti-NDRG1/Cap43 antibody was generated as described previously (5). Other antibodies were purchased as follows: anti-β-actin antibody (Abcam); anti-NIK, anti-TAB1/2, anti-TAK1, anti-inhibitor of κB kinase (IKK) α, anti-IKKβ, anti-IKKγ, anti-p-IκBα, anti-p65, anti-p50, anti-RelB, anti-p52, and anti-ubiquitin antibodies (Cell Signaling Technology); anti-p65 and anti-p50 antibodies for supershift analysis by electromobility shift assay (EMSA; Santa Cruz Biotechnology); anti-Flag M2 antibody (Sigma); and anti-CD68 and anti-neutrophil elastase antibodies (DAKO). Human tumor necrosis factor-α (TNF-α) and MG-132 was purchased from R&D Systems and Calbiochem.

Note: Supplementary data for this article are available at Cancer Research Online (http://cancerres.aacrjournals.org/).

Requests for reprints: Mayumi Ono, Department of Pharmaceutical Oncology, Graduate School of Pharmaceutical Sciences, Kyushu University, 3-1-1 Maidashi, Higashi-ku, Fukuoka 812-8582, Japan. Phone: 81-92-642-6296; Fax: 81-92-642-6296; E-mail: mono@phar.kyushu-u.ac.jp.

doi:10.1158/0008-5472.CAN-08-4882

Plasmid constructs. To obtain full-length cDNA of human IKKβ, PCR was carried out on a SuperScript cDNA library (Invitrogen) using the following primer pairs: 5′-ATGAGCTGGTCACCTTCCCTGACAAC-3′ and 5′-TCATGAGGCCTGCTCCAGGCAGCTG-3′ (IKKβ). The PCR product was ligated into the pGEM-T easy vector (Promega), and Flag-IKKβ was ligated into the p3xFLAG-CMV10 vector (Sigma).

Oligonucleotide microarray analysis. Duplicate samples were prepared for microarray hybridization. Total RNA (2 μg) was reverse transcribed using a GeneChip 3′-Amplification Regents One Cycle cDNA Synthesis kit (Affymetrix) and labeled with Cy5 or Cy3. The labeled cRNA was applied to the oligonucleotide microarray (Human Genome U133 Plus 2.0 Array; Affymetrix), the microarray was scanned on a GeneChip Scanner3000, and the image was analyzed using GeneChip Operating Software version 1 as described previously (15).

Determination of melanoma growth-stimulating activity α/CXCL1, epithelial-derived neutrophil activating protein-78/CXCL5, IL-8/CXCL8, and VEGF-A levels by ELISA. The concentrations of IL-8/CXCL8, VEGF-A, melanoma growth-stimulating activity α (Groα)/CXCL1, and epithelial-derived neutrophil activating protein-78 (ENA-78)/CXCL5 in the homogenized supernatant of mouse xenograft tumors and conditioned medium were measured using commercially available ELISA kits (R&D Systems) in accordance with the manufacturer's instructions.

EMSA. EMSA was done as follows. Nuclear extract (6 μg) was incubated for 15 min at room temperature with a 1×10^4 counts/min ^{32}P-labeled oligonucleotide probe in binding buffer [10 mmol/L HEPES-NaOH (pH 7.9), 1 mmol/L EDTA, 50 mmol/L NaCl, 10% glycerol, 0.1 mg/mL bovine serum albumin, 0.05% NP-40, 0.005 mg/mL DTT, 0.05 mg/mL poly(deoxyinosinic-deoxycytidylic acid)] as described previously (16). The reaction mixtures were separated on a nondenaturing 4% polyacrylamide gel, and radioactivity was detected with a FLA 5000 image analyzer (Fuji Film).

Immunoprecipitations and Western blotting. The cells treated with or without MG-132 (10 μmol/L) under 2% serum condition for 8 h were lysed in lysis buffer [50 mmol/L Tris-HCl (pH 8.0), 250 mmol/L NaCl, 0.3% NP-40, 1 mmol/L EDTA, 10% glycerol, 0.1 mmol/L Na_3VO_4] supplemented with a mixture of protease inhibitors. Lysates were incubated with anti-ubiquitin antibody for 2 h at 4°C and with protein A/G agarose for additional 1 h. After all immunoprecipitates were washed three times with lysis buffer, Western blotting was done with anti-IKKβ antibody as described previously (17). The intensity of the luminescence was quantified using a CCD camera combined with an image analysis system (LAS-1000; Fuji Film).

Animals. All animal experiments were approved by the Ethics of Animal Experiments Committee at Kyushu University Graduate School of Medical Sciences. Male athymic *nu/nu* mice were purchased from Charles River Laboratories and housed in microisolator cages maintained under a 12-h light/dark cycle. Water and food were supplied *ad libitum*. Animals were observed for signs of tumor growth, activity, feeding, and pain in accordance with the guidelines of the Harvard Medical Area Standing Committee on Animals.

Immunohistochemical analysis. MIApaca-2 transfectants were injected subcutaneously into mice (1.0×10^7 cells/0.1 mL/mouse). At day 49 after transplantation of MIApaca-2 transfectants, the tumors were fixed and immunohistochemical analysis was done as described previously (5, 18). All human tissue samples were fixed and embedded in paraffin, and immunohistochemical analysis was done as described previously (5, 18). In all tissue samples, the mean value of the number of infiltrating macrophages and neutrophils and the MVD were calculated from four or five hotspots. All counts were done by three independent observers.

Statistical analysis. Data are expressed as mean ± SD. All calculations (Welch's *t* test, Student's *t* test, and Wilcoxon/Kruskal-Wallis test) were done using JMP version 5.0 (SAS Institute).

Patients and specimens. Surgically respected specimens from 37 patients with pancreatic ductal adenocarcinoma were studied. All patients underwent surgical resection between 1991 and 1998 at the Department of Surgery, Kurume University Hospital. Informed consent was obtained from all patients, and the study protocol was approved by the Ethics Committee of Kurume University.

Results

NDRG1/Cap43 down-regulates the expression of angiogenesis- and inflammation-related genes. To understand how NDRG1/Cap43 modulates tumor angiogenesis and growth in pancreatic cancer cells, we compared the expression profiles of NDRG1/Cap43 transfectant (Cap#11) and the parental low-expression counterpart (Mock#2) of MIApaca-2 cells using a high-density oligonucleotide microarray (Supplementary Table S1).

We selected eight genes predicted to be associated with adhesion, growth, and chemotaxis (Supplementary Table S2). Because our previous study showed that NDRG1/Cap43 overexpression in pancreatic cancer cells reduced the expression of angiogenesis-related factors such as VEGF-A and IL-8/CXCL8 (5), we also selected these genes, the expression of which showed a decrease of ~0.7 (Supplementary Table S2).

We confirmed the expression of NDRG1/Cap43 in two NDRG1/Cap43 transfectants (Cap#11 and Cap#14) and their mock transfectants (Mock#2) of MIApaca-2 cells (Fig. 1*A*). We compared the expression of these genes in high- and low-NDRG1/Cap43-expressing MIApaca-2 cells by quantitative real-time PCR. From the array results, we selected NCAM1, which was up-regulated by NDRG1/Cap43, as a control. The mRNA expression levels of Groα/CXCL1, ENA-78/CXCL5, IL-8/CXCL8, and VEGF-A were significantly decreased in two NDRG1/Cap43 transfectants (Cap#11 and Cap#14) in comparison with Mock#2 cells (Supplementary Fig. S1).

We used ELISA assays to compare protein levels of chemokines among pancreatic cancer cells showing low and high expression of NDRG1/Cap43 (Fig. 1*B*). We observed that Cap#11 and Cap#14 cells showed a marked decrease in the production of Groα/CXCL1 and ENA-78/CXCL5 as well as IL-8/CXCL8.

NDRG1/Cap43 suppresses the NF-κB signaling pathway in pancreatic cancer cells. Representative angiogenic factors such as IL-8/CXCL8 and VEGF-A are regulated by NF-κB (19). We investigated whether NDRG1/Cap43 expression interfered with the NF-κB signaling pathway in pancreatic cancer cells. The phosphorylation of IκBα was activated in Mock#2 cells cultured in the presence of 2% serum compared with Cap#11 and Cap#14 cells (Fig. 1*C, left*). By contrast, in the absence of serum, there appeared to be weak activation of IκBα in Mock#2 cells. However, NDRG1/Cap43 expression level was not affected with or without serum in NDRG1/Cap43 transfectants (Fig. 1*C, left*). Next, we determined the expression levels of proteins related to the NF-κB signaling pathway to examine which molecules are responsible for the difference in the phosphorylation level of IκBα between NDRG1/Cap43 and mock transfectants. Phosphorylation of IκBα is regulated by the IKK complex, which consists of two catalytic subunits, IKKα and IKKβ, and a regulatory component, IKKγ/NEMO. The expression of IKKβ was markedly reduced in Cap#11 and Cap#14 cells compared with Mock#2 cells (Fig. 1*C, middle*). There were no differences in the expression levels of other NF-κB signaling pathway-related proteins (NIK, TAB1/2, TAK1, IKKα, and IKKγ) between NDRG1/Cap43 and mock transfectants, and the expression levels of NF-κB subunits such as p65, p50, RelB, and p52 in Cap#11 and Cap#14 cells were similar to those in Mock#2 cells (Fig. 1*C, right*). Expression of IKKβ mRNA is slightly, but not significantly, decreased in NDRG1/Cap43 transfectants (Supplementary Fig. S2). In Cap#11 and Cap#14 cells, nuclear translocation of p65 was decreased by ~50% to 70% and that of p50 was decreased by ~80% compared with Mock#2, respectively (Fig. 1*D, left*). Expression of p65 and p50 showed only a slight increase in

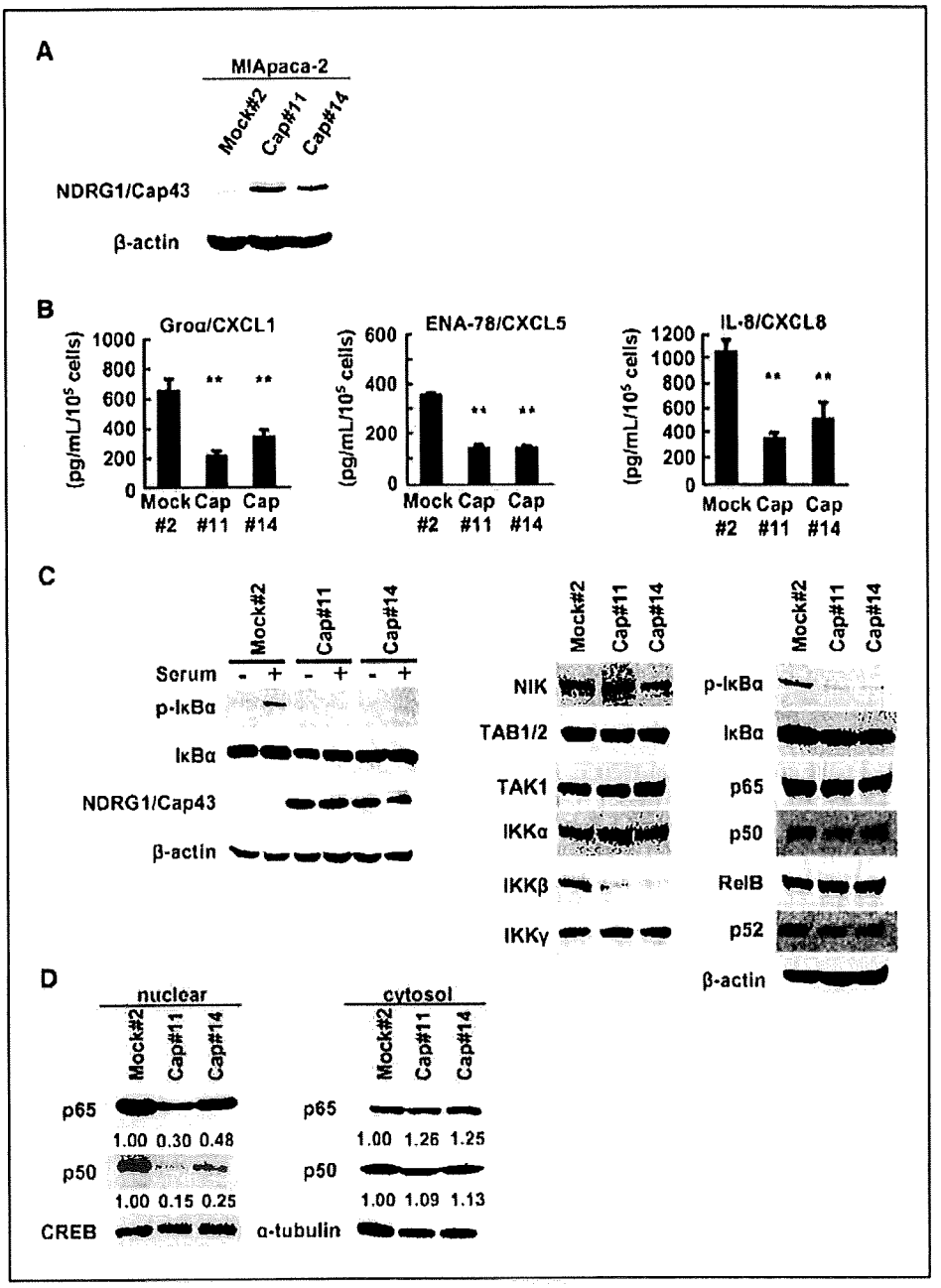

Figure 1. NDRG1/Cap43 reduces expression levels of CXC chemokines and phosphorylation of IκBα in MIApaca-2 cell lines showing low and high NDRG1/Cap43 expression. All experiments, except *A*, were done with 2% serum for 24 h. *A*, Western blot analysis of NDRG1/Cap43 expression in MIApaca-2 transfectants. *B*, ELISA assay analysis of Groα/CXCL1, ENA-78/CXCL5, and IL-8/CXCL8 protein levels in NDRG1/Cap43 and mock transfectants of MIApaca-2 cells. *Columns*, mean of three independent experiments; *bars*, SE. **, $P < 0.01$ versus Mock#2 cells. *C*, phosphorylation of IκBα and NDRG1/Cap43 expression in NDRG1/Cap43 and mock transfectants cultured with or without 2% serum for 24 h was measured by Western blotting (*left*). Western blot analysis of the expression of NF-κB signaling pathway-related proteins using whole-cell lysates prepared from NDRG1/Cap43 and mock transfectants (*middle* and *right*). *D*, Western blot analysis of the expression of p65 and p50 in nuclear (*left*) and cytosol (*right*) extracts prepared from NDRG1/Cap43 and mock transfectants. Levels of protein expression are expressed relative to the level of p65 or p50 protein in Mock#2, which is presented as 1.00.

cytosol fraction of Cap#11 and Cap#14 compared with that of Mock#2 (Fig. 1*D*, *right*).

We next performed EMSA to assess whether NDRG1/Cap43 altered the binding ability of NF-κB. One major shifted protein-DNA complex was observed after incubation of nuclear extracts prepared from Mock#2 cultured with 2% serum for 24 h (Fig. 2*A*). These complexes were specifically competed out with a 2-fold excess of the same unlabeled oligonucleotide but not with an unlabeled TRE and GC-box oligonucleotide. The protein-DNA complex after incubation of nuclear extracts was markedly decreased in Cap#11 and Cap#14 compared with Mock#2 when cultured with 2% serum. When protein-DNA complexes were incubated with antibodies against p65 and p50, supershifted bands were observed in Mock#2 (Fig. 2*A*). We next examined whether the reduced level of p-IκBα could be restored by a potent inflammatory cytokine, TNF-α, in NDRG1/Cap43 transfectants (Fig. 2*B*). TNF-α induced phosphorylation of IκBα in both Cap#11 and Cap#14 at similar levels as their parental counterpart. However, cellular levels of IKKβ in Cap#11 and Cap#14 were not affected by TNF-α. Figure 2*C* shows that TNF-α also restored the expression of IL-8/CXCL8 in Cap#11 and Cap#14 cells to levels comparable with those in Mock#2 cells. Treatment with TNF-α also enhanced the affinity of p65 and p50 for NF-κB binding sites in Cap#11 and Cap#14 at similar levels to those in their parental counterparts (Fig. 2*D*). Taken together, NDRG1/Cap43 was not involved in TNF-α-induced NF-κB signaling pathway.

IKKβ overexpression overcomes NDRG1/Cap43-induced suppression of IκBα phosphorylation and chemokine expression. Expression of IKKβ was decreased in two NDRG1/Cap43 transfectants (Cap#11 and Cap#14). We examined whether exogenous IKKβ expression was able to restore the IκBα phosphorylation in NDRG1/Cap43 transfectants. Expression of IKKβ was augmented in both NDRG1/Cap43 and mock transfectants after transfection of the exogenous IKKβ gene (Fig. 3*A*). The phosphorylation of IκBα was increased in Cap#11 to a level comparable with that in Mock#2. Expression of Groα/CXCL1, ENA-78/CXCL5, and IL-8/CXCL8 was also significantly increased after transfection of IKKβ in Cap#11 cells when there was no apparent difference in the expression levels of these chemokines between empty and IKKβ transfection in Mock#2 (Fig. 3*B*). Expression of VEGF-A was also increased in IKKβ-transfected Cap#11 cells compared with that in empty-transfected Cap#11 cells. We observed that VEFG-A expression was decreased in IKKβ-transfected Mock#2 compared with empty-transfected Mock#2 cells, but the reason for this remains unclear.

IKKβ has been reported to hold a putative ubiquitin-like domain (20). We examined whether the reduced expression of IKKβ protein was restored by proteasome inhibitor, MG-132, in Cap#11 cells. MG-132 inhibited degradation of p-IκBα in both Mock#2 and Cap#11 cells (Fig. 3*C*). Furthermore, expression of IKKβ in Cap#11 cells was restored to similar levels as in Mock#2 cells when treated with MG-132. MG-132 did not significantly affect IKKβ mRNA expression in Mock#2 ($P = 0.65$) and Cap#11 ($P = 0.48$) cells

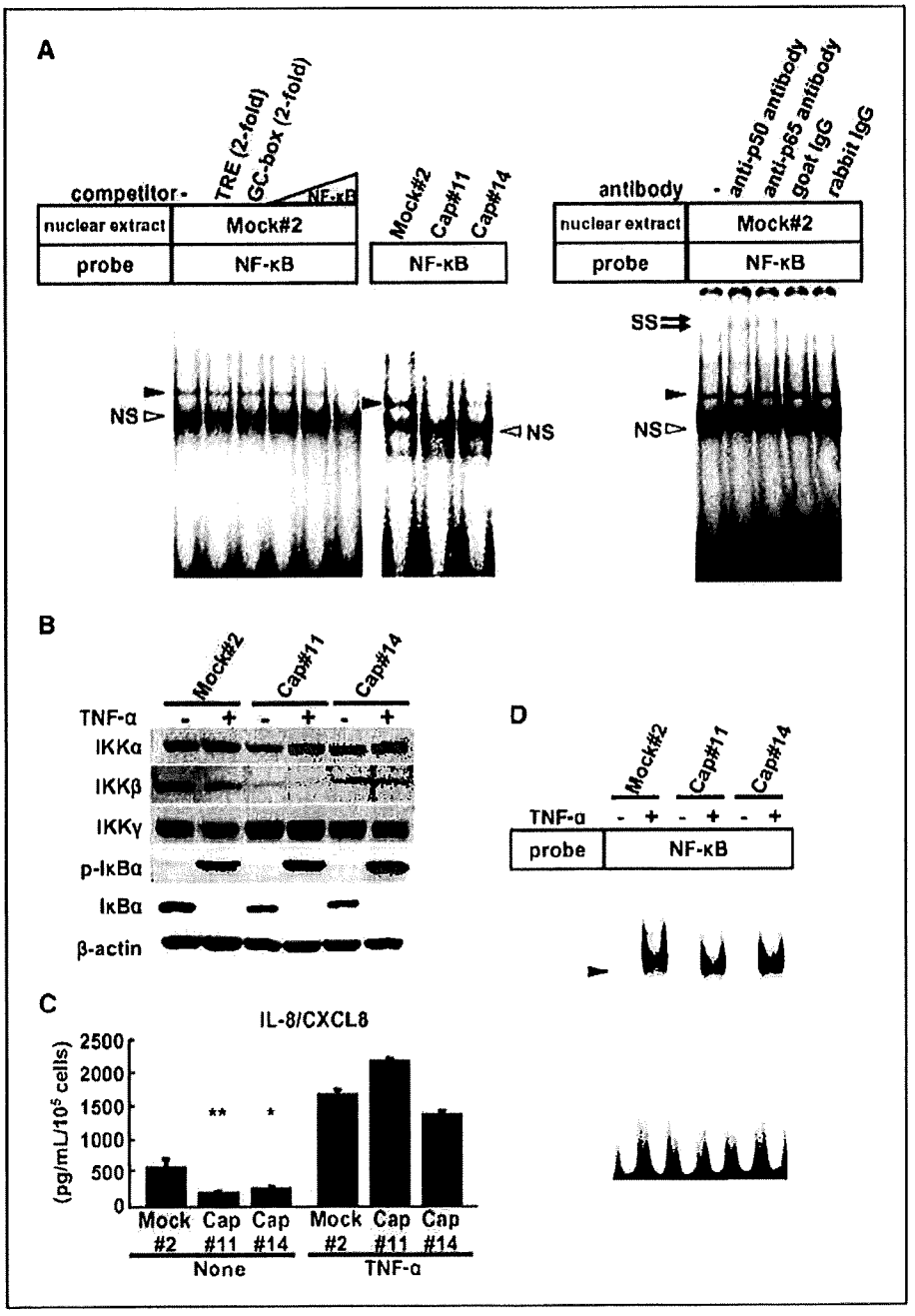

Figure 2. Suppression of binding activity of NF-κB by NDRG1/Cap43. *A*, EMSA using the NF-κB binding oligonucleotide. Nuclear extracts from three transfectants cultured in the presence of 2% serum were incubated with oligonucleotide as described in Materials and Methods. *Black arrowheads*, shifted bands; 0.08-, 0.4-, or 2-fold molar excess of unlabeled oligonucleotide was used as the competitor. A 2-fold molar excess of unlabeled oligonucleotide (TRE and GC-box) was used as a negative control for this competition assay. *Arrows*, positions of the supershifted bands (*SS*); *NS*, nonspecific band (*white arrowheads*). *B*, Western blot analysis of IκBα phosphorylation and expression of IKKα, IKKβ, and IKKγ in NDRG1/Cap43 and mock transfectants under serum-free conditions with or without TNF-α (20 ng/mL) stimulation for 30 min. *C*, ELISA assay analysis of IL-8/CXCL8 protein levels in NDRG1/Cap43 and mock transfectants of MIApaca-2 cells under serum-free conditions with or without TNF-α (20 ng/mL) for 24 h. *Columns*, mean of three independent experiments; *bars*, SE. *, $P < 0.05$; **, $P < 0.01$ versus mock transfectants. *D*, EMSA using the NF-κB binding oligonucleotide with nuclear extracts from three transfectants under serum-free conditions with or without TNF-α (20 ng/mL) for 30 min. *Black arrowheads*, shifted bands.

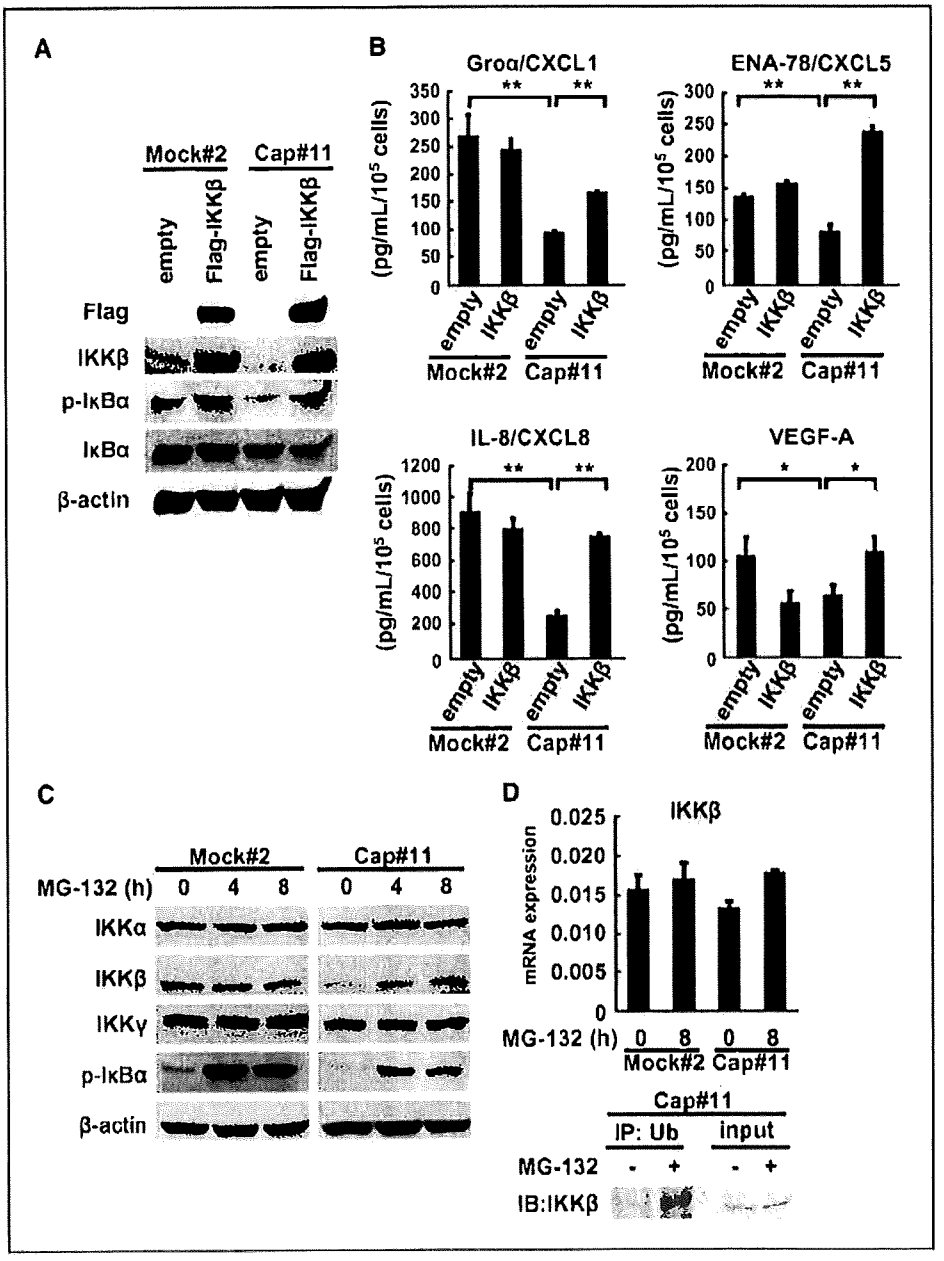

Figure 3. IKKβ overexpression restores the level of p-IκBα and expression of the CXC chemokines and VEGF-A. *A*, expression of the exogenous IKKβ gene and phosphorylation of IκBα in MIApaca-2 transfectants. NDRG1/Cap43 and mock transfectants were transiently transfected with the IKKβ expression vector. At 30 h after IKKβ transfection, the cells were again seeded and cultured for 18 h and then cultured in medium containing 2% serum for 24 h. *B*, ELISA assay analysis of Groα/CXCL1, ENA-78/CXCL5, IL-8/CXCL8, and VEGF-A protein levels in Mock#2 and Cap#11 that were transfected with the IKKβ expression vector. At 48 h after IKKβ transfection, the cells were cultured in medium containing 2% serum for 24 h. *Columns*, mean of three independent experiments; *bars*, SE. *, $P < 0.05$; **, $P < 0.01$ versus empty-transfected Cap#11 cells. *C*, Western blot analysis of IκBα phosphorylation and IKKα, IKKβ, and IKKγ expression in NDRG1/Cap43 and mock transfectants treated with MG-132 (10 μmol/L) in the presence of 2% serum for indicated time. *D*, quantitative real-time PCR analysis of IKKβ mRNA levels in NDRG1/Cap43 and mock transfectants treated with MG-132 (10 μmol/L) in the presence of 2% serum for the indicated time. *Columns*, mean of three independent experiments; *bars*, SE (*top*). Cells were treated with or without MG-132 (10 μmol/L) for 8 h before lysis. Immunoprecipitation was done with anti-ubiquitin (*Ub*) antibody and immunoblotting was with anti-IKKβ antibody (*bottom*).

(Fig. 3*D*, *top*). We further examined whether IKKβ was ubiquitinated or not in the presence of MG-132. As shown in Fig. 3*D* (*bottom*), ubiquitination of IKKβ was shown in Cap#11 cells, suggesting that a proteasomal degradation plays a role in down-regulation of IKKβ in the NDRG/Cap43-expressing cells.

NDRG1/Cap43 suppresses infiltration of inflammatory cells, expression of angiogenesis-related factors, tumor growth, and tumor angiogenesis. Consistent with our previous study (5), there was no difference in growth rates among Mock#2 and Cap#11 cells in culture (Fig. 4*A*). By contrast, tumor growth of Cap#11 was markedly reduced in comparison with Mock#2 in a subcutaneous mouse xenograft model (Fig. 4*B*, *bottom*). Immunoblotting analysis showed that NDRG1/Cap43 protein was consistently and highly expressed in Cap#11 tumors on day 49 after inoculation compared with Mock#2 tumors (Fig. 4*B*, *top*).

NDRG1/Cap43 was found to reduce the expression of chemokines and growth factors that function in chemotaxis of monocytes/macrophages and neutrophils (Fig. 1*B*; Supplementary Fig. S1). Mock#2 and Cap#11 tumor sections were further analyzed by immunohistochemistry for expression of microvessels (CD31), macrophages (F4/80), and neutrophils (Gr-1; Fig. 4*C*, *top*). MVD staining showed a markedly higher number of tumor neovessels in Mock#2 tumors than in Cap#11 tumors on day 49 after implantation (Fig. 4*C*, *bottom*). There appeared to be much lower infiltration of F4/80-positive macrophages and also Gr-1-positive infiltrating neutrophils in the stroma of Cap#11 tumors compared with that of Mock#2 tumors (Fig. 4*C*, *bottom*). NDRG1/Cap43 expression was thus closely associated with decreased MVD and also with a decreased number of infiltrating macrophages and neutrophils in mouse xenograft tumors. Expression of IL-8/CXCL8 and

VEGF-A was significantly reduced in Cap#11 tumors compared with Mock#2 tumors (Fig. 4*D*), suggesting that reduced expression of such chemokines and growth factors was continuously maintained during tumor growth in this mouse xenograft model.

Association of NDRG1/Cap43 expression level with infiltrating inflammatory cells in tumors of pancreatic cancer patients. Expression of NDRG1/Cap43 was previously shown to be inversely correlated with MVD in the tumors of patients with pancreatic cancer (5). Based on the expression level of NDRG1/Cap43 in resected specimens from 37 patients with pancreatic ductal adenocarcinoma, we divided them into two groups: NDRG1/Cap43 positive (n = 18) and NDRG1/Cap43 negative (n = 19). Supplementary Table S3 shows the association between NDRG1/Cap43 expression and clinicopathologic variables such as age, gender, depth of invasion, lymph node metastasis, and pathologic stage in patients with pancreatic ductal adenocarcinoma. High NDRG1/Cap43 expression was significantly correlated with invasion depth (Supplementary Table S3).

In the human tumor stroma, some cases showed a lower number of infiltrating $CD68^+$ macrophages/monocytes in NDRG1/Cap43-positive pancreatic cancer (Fig. 5*A*, *a* and *b*), whereas others showed a higher number of infiltrating $CD68^+$ macrophages/monocytes in NDRG1/Cap43-negative pancreatic cancer (Fig. 5*A*, *c* and *d*). Quantitative analysis indicated that the number of infiltrating macrophages/monocytes was relatively higher in patients with NDRG1/Cap43-negative tumors than in those with NDRG1/Cap43-positive tumors (Fig. 5*A*, *right*), the mean number of infiltrating macrophages/monocytes being 97.5 and 62.3, respectively. However, similar numbers of infiltrating neutrophils were observed in the tumor stroma of patients with NDRG1/Cap43-positive and

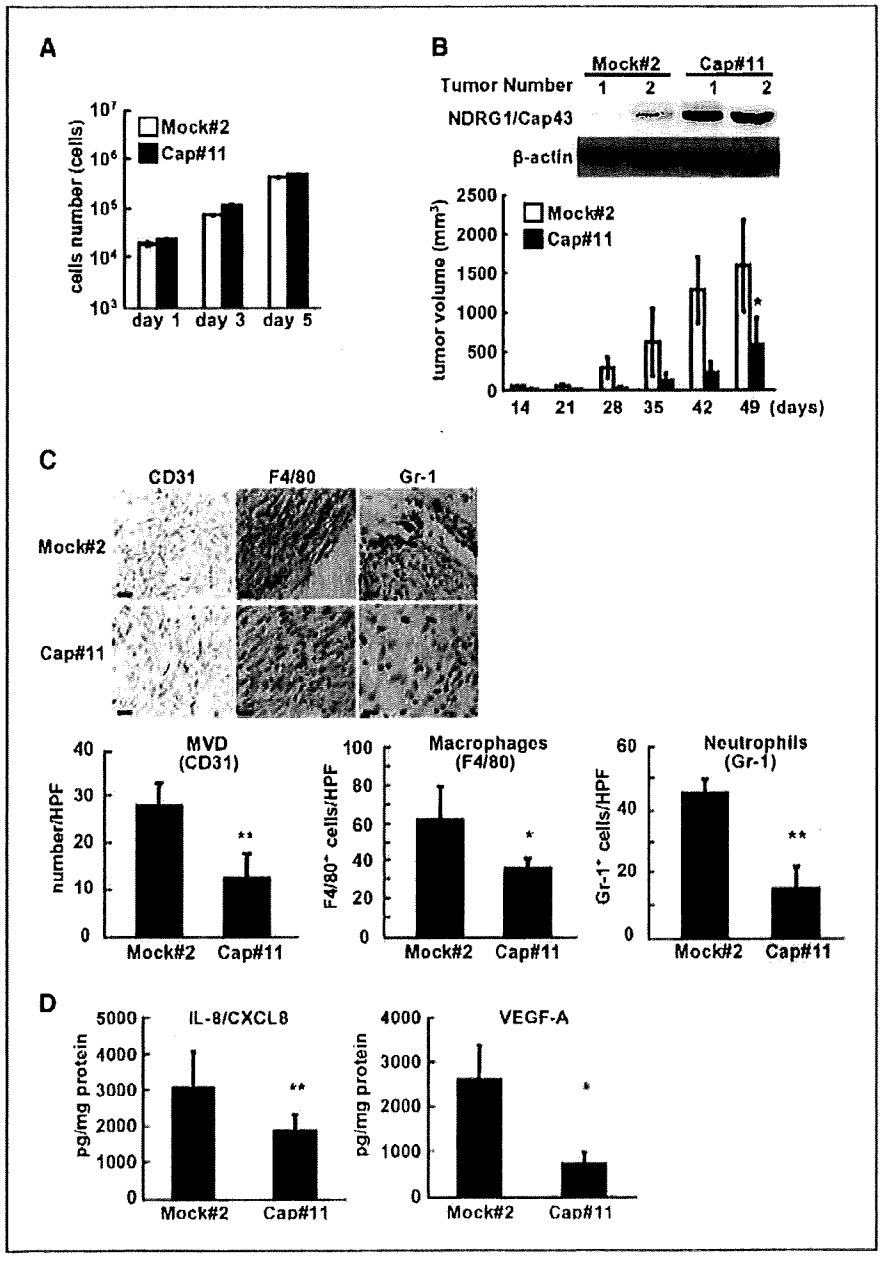

Figure 4. NDRG1/Cap43 represses MVD and the number of infiltrating macrophages or neutrophils in mouse subcutaneous tumors. *A*, comparison of cell proliferation in MIApaca-2 transfectant cells (Mock#2 and Cap#11). Cells were seeded on day 0 at 1.0×10^4 per well and cultured in DMEM with 10% serum. Cell growth was measured on days 1, 3, and 5. *Columns*, mean of three independent experiments; *bars*, SE. *B*, Western blot analysis of NDRG1/Cap43 expression in tumors comprising Mock#2 or Cap#11 cells on day 49 (*top*). *Columns*, mean tumor volumes; *bars*, SE. Tumor volumes were determined every week after tumor implantation (n = 5 or 6; *bottom*). *C*, immunohistochemical analysis. Representative photographs of tumor sections stained with the anti-CD31, anti-F4/80, and anti-Gr-1 antibodies from Mock#2 and Cap#11 xenografts on day 49. *Bar*, 25 μm (*top*). Mean MVD for tumor sections from Mock#2 and Cap#11 xenografts on day 49 was determined by counting the number of $CD31^+$ vessels in the tumors. Mean numbers of infiltrating macrophages and neutrophils in tumor sections from Mock#2 and Cap#11 xenografts on day 49 were determined by counting the intensity of F4/80- or Gr-1-positive cells in the tumor stroma. *Columns*, mean; *bars*, SE (n = 5; *bottom*). *HPF*, high-power field. *D*, ELISA assay analysis of human IL-8/CXCL8 and VEGF-A protein levels in Mock#2 and Cap#11 tumors. *Columns*, mean; *bars*, SE (n = 4). *, $P < 0.05$; **, $P < 0.01$ versus Mock#2 tumors.

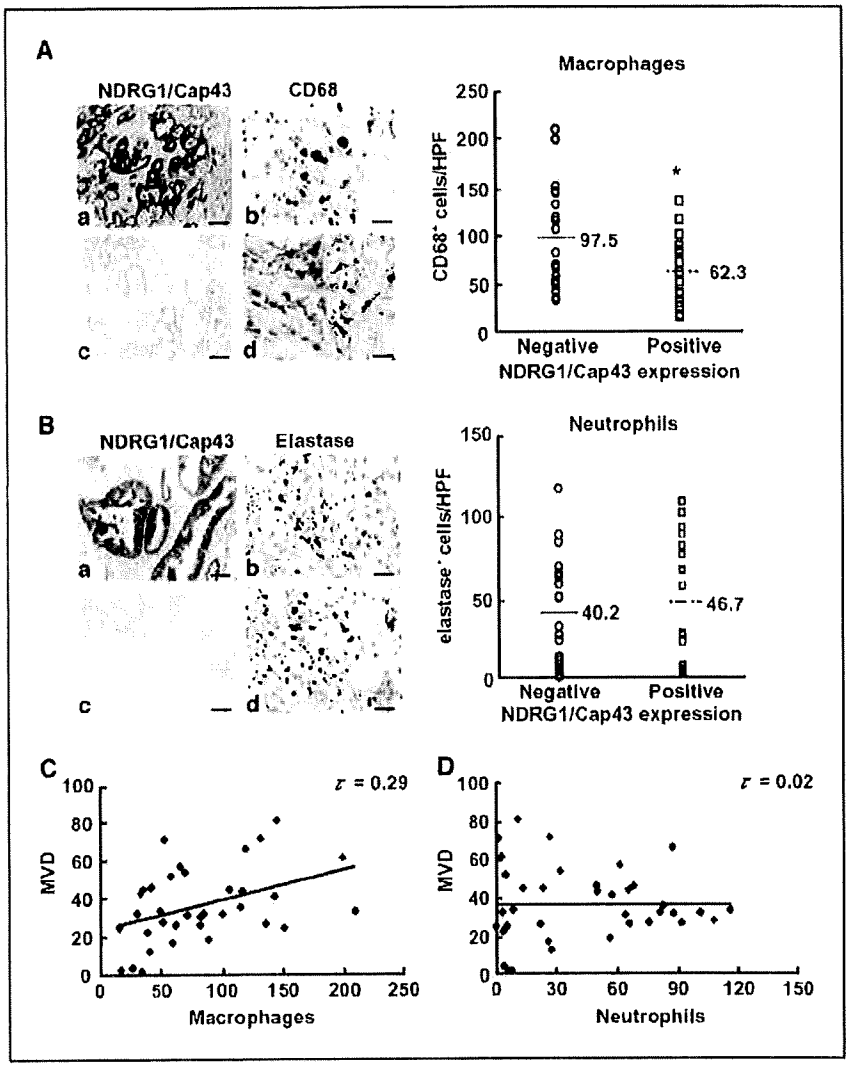

Figure 5. NDRG1/Cap43 expression levels and numbers of infiltrating inflammatory cells in human pancreatic cancer. *A*, immunohistochemical analysis of macrophages in tumor stroma using the anti-NDRG1/Cap43 antibody and anti-CD68 antibody. Representative photographs showing low infiltration of macrophages in NDRG1/Cap43-positive specimens (*a* and *b*). Representative photographs showing high infiltration of macrophages in NDRG1/Cap43-negative specimens (*c* and *d*). *Bar*, 50 μm (*a* and *c*) and 25 μm (*b* and *d*). Correlation between NDRG1/Cap43 expression levels and numbers of infiltrating macrophages. Mean number of infiltrating macrophages was 97.5 in NDRG1/Cap43-negative specimens ($n = 19$) and 62.3 in NDRG1/Cap43-positive specimens ($n = 18$; *right*). *, $P < 0.05$. *B*, immunohistochemical analysis of neutrophils in tumor stroma using an anti-NDRG1/Cap43 antibody and anti-elastase antibody. Representative photographs of neutrophils infiltration in NDRG1/Cap43-positive specimens (*a* and *b*) and NDRG1/Cap43-negative specimens (*c* and *d*). Correlation between NDRG1/Cap43 expression level and number of infiltrating neutrophils. Mean number of infiltrating neutrophils was 40.2 in NDRG1/Cap43-negative specimens and 46.7 in NDRG1/Cap43-positive specimens (*right*). *C* and *D*, correlation between MVD and number of infiltrating macrophages or neutrophils in patients with pancreatic ductal adenocarcinoma ($n = 37$). $r = 0.29$ and 0.02, Kendall correlation coefficient.

NDRG1/Cap43-negative pancreatic cancer (Fig. 5*B*). Quantitative analysis showed that the mean number of infiltrating neutrophils was 40.2 in NDRG1/Cap43-negative specimens and 46.7 in NDRG1/Cap43-positive specimens, with no significant difference (Fig. 5*B*, *right*).

Our previous study showed that NDRG1/Cap43 expression levels were inversely correlated with MVD (5). Therefore, we further examined whether infiltration of macrophages/monocytes and neutrophils was associated with MVD in patients with NDRG1/Cap43-positive and NDRG1/Cap43-negative pancreatic cancer ($n = 37$). The number of infiltrating macrophages/monocytes was positively correlated with MVD (Fig. 5*C*; $P < 0.05$). However, there was no correlation between the number of infiltrating neutrophils and the MVD (Fig. 5*D*).

Discussion

We reported previously that NDRG1/Cap43 overexpression suppressed the expression of VEGF-A, IL-8/CXCL8, and matrix metalloproteinase-9 in pancreatic cancer cells (5). In the present study, we showed that NDRG1/Cap43 down-regulated the expression of several other genes, including chemoattractants for inflammatory cells. We also observed that decreased expression of IL-8/CXCL8 and VEGF-A in mouse tumors was associated with high expression of NDRG1/Cap43. These chemoattractants down-regulated by NDRG1/Cap43 had chemotactic effects on monocytes/macrophages and neutrophils. Our results showed that overexpression of NDRG1/Cap43 resulted in marked decrease in infiltration of macrophages and neutrophils in xenograft models.

One critical step in progression from a benign to a malignant state is angiogenesis. Infiltration of activated fibroblasts (21), macrophages/monocytes (22), and neutrophils (23) is expected to play a key role in the angiogenic switch of cancer (23–25). From our laboratory, we have also reported that infiltration of macrophages in the tumor stroma markedly promoted angiogenesis through the secretion of various proangiogenic cytokines and extracellular matrix-degrading proteases (18, 26–29). Groα/CXCL1, ENA-78/CXCL5, and IL-8/CXCL8 play an important role in tumor-associated angiogenesis and tumorigenesis in cancers of the kidney, pancreas, head and neck, and lung (30–33). Also, expression of CXC chemokines and VEGF-A would thus be expected to be closely involved in NDRG1/Cap43-induced suppression of tumor angiogenesis (Fig. 6). However, it is important to elucidate in more detail the underlying mechanism by which cytokines and growth

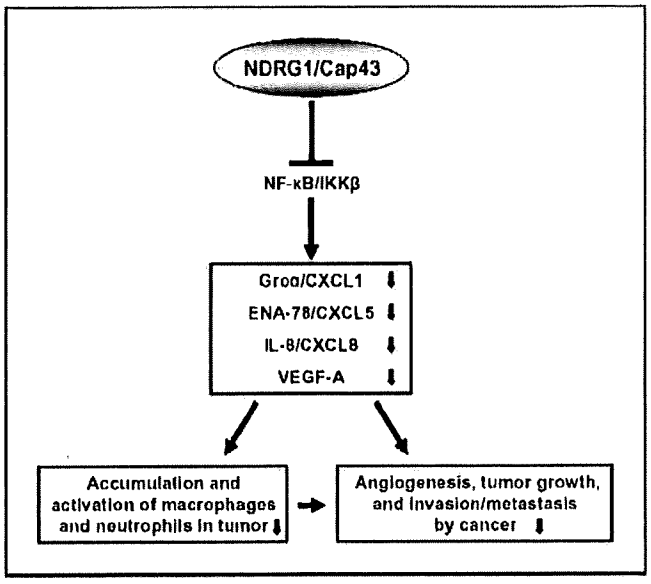

Figure 6. NDRG1/Cap43 plays a critical role as an antiangiogenic regulator through modulation of the tumor microenvironment in pancreatic cancer. NDRG1/Cap43 attenuates activation of the NF-κB/IKKβ signaling, resulting in decreased expression of CXC chemokines (Groα/CXCL1, ENA-78/CXCL5, and IL-8/CXCL8) and VEGF-A. NDRG1/Cap43 might thus remodel the tumor microenvironment by affecting the accumulation of inflammatory cells (macrophages and neutrophils), tumor angiogenesis, and tumor growth.

factors are directly involved in the NDRG1/Cap43-dependent suppression of inflammatory cell infiltration and angiogenesis.

Constitutive activation of NF-κB signaling pathway has been reported in many cancers, including pancreatic cancer (34). Fujioka and colleagues reported that pancreatic cancer cells expressing phosphorylation-defective IκBα showed decreased tumorigenicity in an orthotopic nude mouse model (35). In this mouse model, deletion of IKKβ in intestinal epithelial cells led to a decrease in tumor incidence without affecting tumor size (36). These studies suggested that the IKKβ-NF-κB signaling pathway plays an important role in tumor development.

In our present study, NDRG1/Cap43 reduced the expression of p-IκBα and its upstream regulator IKKβ in pancreatic cancer cells. However, we found no apparent phosphorylation of IKKα and IKKβ in NDRG1/Cap43 and mock transfectants under 2% serum condition (data not shown), suggesting that decreased expression of IKKβ is responsible for the loss of p-IκBα in NDRG1/Cap43 transfectants. The loss of p-IκBα results in reduction of both nuclear translocation of p65 and p50 and their binding to the NF-κB motif. NDRG1/Cap43-induced suppression of IKKβ was almost completely restored by a proteasome inhibitor. Introduction of an exogenous IKKβ gene was able to restore IκBα phosphorylation and expression of Groα/CXCL1, ENA-78/CXCL5, IL-8/CXCL8, and VEGF-A in NDRG1/Cap43 transfectants. In this study, we also found ubiquitination of IKKβ in NDRG1/Cap43 transfectant. A relevant study by May and colleagues showed that a ubiquitin-like domain of IKKβ is required for its functional activation (20). Taken together, the IKKβ-NF-κB pathway is expected to be attenuated by NDRG1/Cap43, resulting in decreased expression of angiogenesis and chemotaxis-related factors (see Fig. 6).

In various solid human tumors, an increase in the number of infiltrating tumor-associated macrophages has been shown to be closely associated with not only prognosis but also tumor angiogenesis (29, 37, 38). In our present study, a significantly decreased number of macrophages was also observed in clinical specimens of pancreatic cancer showing relatively higher NDRG1/Cap43 expression. The number of infiltrating macrophages was correlated with neovascularization in patients with pancreatic cancer. By contrast, we did not observe any significant difference in the number of infiltrating neutrophils between human pancreatic cancers showing low and high expression of NDRG1/Cap43. As shown in Fig. 4, in mouse xenograft models, chemotaxis of neutrophils and macrophages/monocytes was suppressed in Cap#11 xenograft. By contrast, in clinical specimens of pancreatic cancer, infiltration of macrophages, but not neutrophils, was significantly associated with higher NDRG1/Cap43 expression. It remains unclear why NDRG1/Cap43 has no effect on the infiltration of neutrophils in clinical specimens of pancreatic cancer, and this question requires further study, focusing particularly on pancreatic cancer at earlier stages.

In conclusion, this study has shown that NDRG1/Cap43 decreases the expression of IKKβ and the NF-κB signaling pathway. As a consequence, NDRG1/Cap43 decreases the expression of chemoattractants such as CXC chemokines and VEGF-A for inflammatory cells, leading to a marked decrease in the recruitment of macrophages and/or neutrophils, along with angiogenesis suppression, in xenograft models. Therefore, NDRG1/Cap43 could be a potent biomarker for modulation of the tumor stroma in pancreatic cancer.

Disclosure of Potential Conflicts of Interest

No potential conflicts of interest were disclosed.

Acknowledgments

Received 12/22/08; revised 3/12/09; accepted 4/17/09; published OnlineFirst 6/2/09.

Grant support: Grants-in-aid for Scientific Research in Priority Areas of Cancer from the Ministry of Education Culture, Sports Science, and Technology of Japan (M. Ono), Third-Term Comprehensive Control Research for Cancer from the Ministry of Health, Labor and Welfare, Japan (M. Kuwano), and Formation of Innovation Center for Fusion of Advanced Technologies, Kyushu University (M. Ono and M. Kuwano), and JSPS-Asia Core Program (M. Ono).

The costs of publication of this article were defrayed in part by the payment of page charges. This article must therefore be hereby marked *advertisement* in accordance with 18 U.S.C. Section 1734 solely to indicate this fact.

We thank Drs. K. Matsuo, T. Utsugi (Hanno Research Center for Taiho Parmaceutical), Y. Maruyama, and Y. Basaki (Kyushu University) for fruitful discussions.

References

1. Berger JC, Vander Griend DJ, Robinson VL, Hickson JA, Rinker-Schaeffer CW. Metastasis suppressor genes: from gene identification to protein function and regulation. Cancer Biol Ther 2005;4:805–12.
2. Kovacevic Z, Richardson DR. The metastasis suppressor, Ndrg-1: a new ally in the fight against cancer. Carcinogenesis 2006;27:2355–66.
3. Guan RJ, Ford HL, Fu Y, Li Y, Shaw LM, Pardee AB. Drg-1 as a differentiation-related, putative metastatic suppressor gene in human colon cancer. Cancer Res 2002;60:749–55.
4. Bandyopadhyay S, Pai SK, Gross SC, et al. The Drg-1 gene suppresses tumor metastasis in prostate cancer. Cancer Res 2003;63:1731–6.
5. Maruyama Y, Ono M, Kawahara A, et al. Tumor growth suppression in pancreatic cancer by a putative metastasis suppressor gene Cap43/NDRG1/Drg-1 through modulation of angiogenesis. Cancer Res 2006; 66:6233–42.
6. Fotovati A, Fujii T, Yamaguchi M, et al. 17β-Estradiol induces down-regulation of Cap43/NDRG1/Drg-1, a putative differentiation-related and metastasis suppressor gene, in human breast cancer cells. Clin Cancer Res 2006;12:3010–8.
7. Bandyopadhyay S, Pai SK, Hirota S, et al. Role of the

putative tumor metastasis suppressor gene Drg-1 in breast cancer progression. Oncogene 2004;23:5675–81.
8. Ando T, Ishiguro H, Kimura M, et al. Decreased expression of NDRG1 is correlated with tumor progression and poor prognosis in patients with esophageal squamous cell carcinoma. Dis Esophagus 2006;19:454–8.
9. Koshiji M, Kumamoto K, Morimura K, et al. Correlation of N-myc downstream-regulated gene 1 expression with clinical outcomes of colorectal cancer patients of different race/ethnicity. World J Gastroenterol 2007;213:2803–10.
10. Fukahori S, Yano H, Tsuneoka M, et al. Immunohistochemical expressions of Cap43 and Mina53 proteins in neuroblastoma. J Pediatr Surg 2007;42:1831–40.
11. Chua MS, Sun H, Cheung ST, et al. Overexpression of NDRG1 is an indicator of poor prognosis in hepatocellular carcinoma. Mod Pathol 2007;20:76–83.
12. Nishio S, Ushijima K, Tsuda N, et al. Cap43/NDRG1/Drg-1 is a molecular target for angiogenesis and a prognostic indicator in cervical adenocarcinoma. Cancer Lett 2008;264:36–43.
13. Nishie A, Masuda K, Otsubo M, et al. High expression of the Cap43 gene in infiltrating macrophages of human renal cell carcinomas. Clin Cancer Res 2001;7:2145–51.
14. Masuda K, Ono M, Okamoto M, et al. Downregulation of Cap43 gene by von Hippel-Lindau tumor suppressor protein in human renal cancer cells. Int J Cancer 2003;105:803–10.
15. Basaki Y, Hosoi F, Oda Y, et al. Akt-dependent nuclear localization of Y-box-binding protein 1 in acquisition of malignant characteristics by human ovarian cancer cells. Oncogene 2006;26:2736–46.
16. Izumi H, Ise T, Murakami T, et al. Structural and functional characterization of two human V-ATPase subunit gene promoters. Biochim Biophys Acta 2003;1628:97–104.
17. Ono M, Hirata A, Kometani T, et al. Sensitivity to gefitinib (Iressa, ZD1839) in non-small cell lung cancer cell lines correlates with dependence on the epidermal growth factor (EGF) receptor/extracellular signal-regulated kinase 1/2 and EGF receptor/Akt pathway for proliferation. Mol Cancer Ther 2004;3:465–72.
18. Nakao S, Kuwano T, Tsutsumi-Miyahara C, et al. Infiltration of COX-2-expressing macrophages is a prerequisite for IL-1β-induced neovascularization and tumor growth. J Clin Invest 2005;115:2979–91.
19. Maeda S, Omata M. Inflammation and cancer: role of nuclear factor-κB activation. Cancer Sci 2008;99:836–42.
20. May MJ, Larsen SE, Shim JH, Madge LA, Ghosh S. A novel ubiquitin-like domain in IκB kinase β is required for functional activity of the kinase. J Biol Chem 2004;279:45528–39.
21. Orimo A, Gupta PB, Sgroi DC, et al. Stromal fibroblasts present in invasive human breast carcinomas promote tumor growth and angiogenesis through elevated SDF-1/CXCL12 secretion. Cell 2005;121:335–48.
22. Condeelis J, Pollard JW. Macrophages: obligate partners for tumor cell migration, invasion, and metastasis. Cell 2006;124:263–6.
23. Nozawa H, Chiu C, Hanahan D. Infiltrating neutrophils mediate the initial angiogenic switch in a mouse model of multistage carcinogenesis. Proc Natl Acad Sci U S A 2006;103:12493–8.
24. Mahadevan D, Von Hoff DD. Tumor-stroma interactions in pancreatic ductal adenocarcinoma. Mol Cancer Ther 2007;6:1186–97.
25. Ardi VC, Kupriyanova TA, Deryugina EI, Quigley JP. Human neutrophils uniquely release TIMP-free MMP-9 to provide a potent catalytic stimulator of angiogenesis. Proc Natl Acad Sci U S A 2007;104:20262–7.
26. Torisu H, Ono M, Kiryu H, et al. Macrophage infiltration correlates with tumor stage and angiogenesis in human malignant melanoma: possible involvement of TNFα and IL-1α. Int J Cancer 2000;85:182–8.
27. Kuwano T, Nakao S, Yamamoto H, et al. Cyclooxygenase 2 is a key enzyme for inflammatory cytokine-induced angiogenesis. FASEB J 2004;18:300–10.
28. Kimura YN, Watari K, Fotovati A, et al. Inflammatory stimuli from macrophages and cancer cells synergistically promote tumor growth and angiogenesis. Cancer Sci 2007;98:2009–18.
29. Ono M. Molecular links between tumor angiogenesis and inflammation: inflammatory stimuli of macrophages and cancer cells as targets for therapeutic strategy. Cancer Sci 2008;99:1501–6.
30. Pöld M, Zhu LX, Sharma S, et al. Cyclooxygenase-2-dependent expression of angiogenic CXC chemokines ENA-78/CXC ligand (CXCL) 5 and interleukin-8/CXCL8 in human non-small cell lung cancer. Cancer Res 2004;64:1853–60.
31. Mestas J, Burdick MD, Reckamp K, Pantuck A, Figlin RA, Strieter RM. The role of CXCR2/CXCR2 ligand biological axis in renal cell carcinoma. J Immunol 2005;175:5351–7.
32. Wente MN, Keane MP, Burdick MD, et al. Blockade of the chemokine receptor CXCR2 inhibits pancreatic cancer cell-induced angiogenesis. Cancer Lett 2006;241:221–7.
33. Miyazaki H, Patel V, Wang H, Edmunds RK, Gutkind JS, Yeudall WA. Down-regulation of CXCL5 inhibits squamous carcinogenesis. Cancer Res 2006;66:4279–84.
34. Zhang Z, Rigas B. NF-κB, inflammation and pancreatic carcinogenesis: NF-κB as a chemoprevention target. Int J Oncol 2006;29:185–92.
35. Fujioka S, Sclabas GM, Schmidt C, et al. Inhibition of constitutive NF-κB activity by IκBαM suppresses tumorigenesis. Oncogene 2003;22:1365–70.
36. Greten FR, Eckmann L, Greten TF, et al. IKKβ links inflammation and tumorigenesis in a mouse model of colitis-associated cancer. Cell 2004;118:285–96.
37. Bingle L, Brown NJ, Lewis CE. The role of tumor-associated macrophages in tumor progression: implications for new anticancer therapies. J Pathol 2002;196:254–65.
38. Chen JJ, Yao PL, Yuan A, et al. Up-regulation of tumor interleukin-8 expression by infiltrating macrophages: its correlation with tumor angiogenesis and patient survival in non-small cell lung cancer. Clin Cancer Res 2003;9:729–37.

Published Online First on September 8, 2009 as 10.1158/0008-5472.CAN-09-1289

Priority Report

mTOR Signal and Hypoxia-Inducible Factor-1α Regulate CD133 Expression in Cancer Cells

Kazuko Matsumoto,[1] Tokuzo Arao,[1] Kaoru Tanaka,[1] Hiroyasu Kaneda,[1] Kanae Kudo,[1] Yoshihiko Fujita,[1] Daisuke Tamura,[1] Keiichi Aomatsu,[1] Tomohide Tamura,[3] Yasuhide Yamada,[3] Nagahiro Saijo,[2] and Kazuto Nishio[1]

[1]Department of Genome Biology, [2]Kinki University School of Medicine, Osaka-Sayama, Osaka, Japan; and [3]Department of Medical Oncology, National Cancer Center Hospital, Chuo-ku, Tokyo, Japan

Abstract

The underlying mechanism regulating the expression of the cancer stem cell/tumor-initiating cell marker CD133/prominin-1 in cancer cells remains largely unclear, although knowledge of this mechanism would likely provide important biological information regarding cancer stem cells. Here, we found that the inhibition of mTOR signaling up-regulated CD133 expression at both the mRNA and protein levels in a CD133-overexpressing cancer cell line. This effect was canceled by a rapamycin-competitor, tacrolimus, and was not modified by conventional cytotoxic drugs. We hypothesized that hypoxia-inducible factor-1α (HIF-1α), a downstream molecule in the mTOR signaling pathway, might regulate CD133 expression; we therefore investigated the relation between CD133 and HIF-1α. Hypoxic conditions up-regulated HIF-1α expression and inversely down-regulated CD133 expression at both the mRNA and protein levels. Similarly, the HIF-1α activator deferoxamine mesylate dose-dependently down-regulated CD133 expression, consistent with the effects of hypoxic conditions. Finally, the correlations between CD133 and the expressions of HIF-1α and HIF-1β were examined using clinical gastric cancer samples. A strong inverse correlation ($r = -0.68$) was observed between CD133 and HIF-1α, but not between CD133 and HIF-1β. In conclusion, these results indicate that HIF-1α down-regulates CD133 expression and suggest that mTOR signaling is involved in the expression of CD133 in cancer cells. Our findings provide a novel insight into the regulatory mechanisms of CD133 expression via mTOR signaling and HIF-1α in cancer cells and might lead to insights into the involvement of the mTOR signal and oxygen-sensitive intracellular pathways in the maintenance of stemness in cancer stem cells. [Cancer Res 2009;69(18):7160–4]

Introduction

The CD133/prominin-1 protein is a five-transmembrane molecule expressed on the cell surface that is widely regarded as a stem cell marker. Growing evidence indicates that CD133 can be used as a cell marker for cancer stem cells or tumor-initiating cells in colon cancer, prostate cancer, pancreatic cancer, hepatocellular carcinoma, neural tumors, and renal cancer (1). Strict regulatory mechanisms governing CD133 expression are thought to be deeply related to inherent cancer stemness; however, such mechanisms remain largely unclear, especially in cancer cells. In brain tumors, the Hedgehog (2), bone morphogenetic protein (3), and Notch (4) signaling pathways have been implicated in the control of CD133+ cancer stem cell function.

Some investigators have shown a relation between hypoxia and CD133 expression in brain tissue. The percentage of CD133-expressing cells was found to increase in a glioma cell line cultured under hypoxic conditions (5), and mouse fetal cortical precursors cultured under normoxic conditions exhibited a reduction in CD133(hi)CD24(lo) multipotent precursors and the failure of the remaining CD133(hi)CD24(lo) cells to generate glia (6). With the exception of these studies in brain tissue, however, data on the expression of CD133 and the involvement of hypoxia and other signaling pathways in cancer cells remains limited.

Several reports have indicated that mTOR is a positive regulator of hypoxia-inducible factor (HIF) expression and activity (7), and the inhibition of HIF-mediated gene expression is considered to be related to the antitumor activity of mTOR inhibitors in renal cell carcinoma (8). We found that mTOR signaling was involved in CD133 expression in gastric and colorectal cancer cells. Thus, we investigated the regulatory mechanism of CD133 in cancer cells.

Materials and Methods

Reagents. 5-Fluorouracil, irinotecan (CPT-11), and rapamycin were purchased from Sigma-Aldrich. Gemcitabine was provided by Eli Lilly. Tacrolimus (LKT Laboratories), LY294002 and wortmannin (Cell Signaling Technology), and deferoxamine mesylate (DFO; Sigma-Aldrich) were purchased from the indicated companies.

Cell cultures and hypoxic conditions. All of the 28 cell lines used in this study were maintained in RPMI 1640 (Sigma) supplemented with 10% heat-inactivated fetal bovine serum (Life Technologies), except for LoVo (F12; Nissui Pharmaceutical), WiDr, IM95, and HEK293 (DMEM; Nissui Pharmaceutical), and Huvec (Humedia; Kurabo). Hypoxic conditions (0.1% O_2) were achieved using the AnaeroPouch-Anaero (Mitsubishi Gas Chemical) with monitoring using an oxygen indicator.

Real-time reverse transcription-PCR. The methods were previously described (9). The primers used for the real-time reverse transcription-PCR (RT-PCR) were as follows: CD133, forward 5′-AGT GGC ATC GTG CAA ACC TG-3′ and reverse 5′-CTC CGA ATC CAT TCG ACG ATA GTA-3′; glyceraldehyde-3-phosphate dehydrogenase (GAPD), forward 5′-GCA CCG TCA AGG CTG AGA AC-3′ and reverse 5′-ATG GTG GTG AAG ACG CCA GT-3′. GAPD was used to normalize the expression levels in the subsequent quantitative analyses.

Clinical samples. The mRNA expression levels of CD133, HIF-1α, and HIF-1β in gastric cancer specimens were obtained from previously published microarray data (9).

Note: Supplementary data for this article are available at Cancer Research Online (http://cancerres.aacrjournals.org/).

K. Matsumoto and T. Arao contributed equally to this work.

Requests for reprints: Kazuto Nishio, Department of Genome Biology, Kinki University School of Medicine, 377-2 Ohno-higashi, Osaka-Sayama, Osaka 589-8511, Japan. Phone: 81-72-366-0221; Fax: 81-72-366-0206; E-mail: knishio@med.kindai.ac.jp.

doi:10.1158/0008-5472.CAN-09-1289

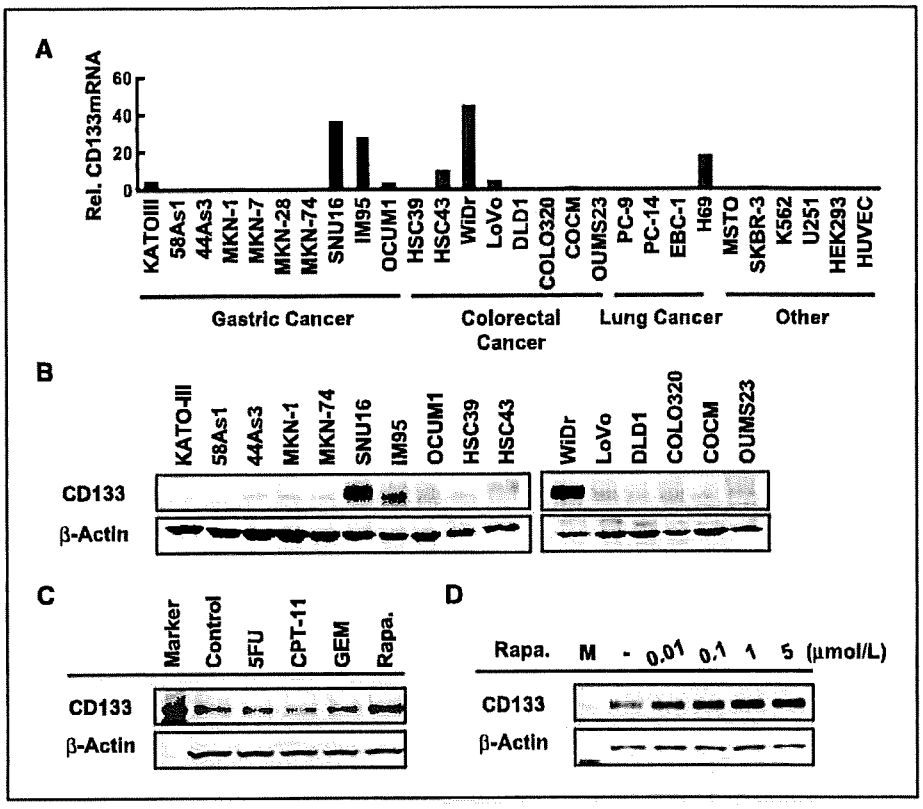

Figure 1. Rapamycin up-regulates CD133 expression. *A*, the mRNA expression levels of CD133 were examined using real-time RT-PCR in 26 cancer cell lines. *B*, the protein expressions of CD133 were determined using Western blotting in 16 gastric and colorectal cancer cell lines. *C*, Western blot of CD133 expression in WiDr cells exposed to cytotoxic drugs [1 μmol/L of 5-fluorouracil (*5-FU*), CPT-11, and gemcitabine (*GEM*)] and rapamycin (1 μmol/L) for 48 h. Note that only rapamycin up-regulates CD133 expression. *D*, WiDr cells were exposed to rapamycin at the indicated concentrations (0, 0.01, 0.1, 1, and 5 μmol/L) for 48 h. Rapamycin dose-dependently up-regulated CD133 expression. *Rel. CD133 mRNA*, normalized mRNA expression levels (CD133/GAPD × 10^4); *Rapa.*, rapamycin.

Immunoblotting. A Western blot analysis was performed as described previously (10). The experiment was performed in triplicate. The following antibodies were used: monoclonal CD133 antibody (W6B3C1; Miltenyi Biotec), rabbit polyclonal HIF-1α antibody (Novus Biologicals, Inc.), β-actin antibody, and HRP-conjugated secondary antibody (Cell Signaling Technology).

Results

Inhibition of the mTOR signal up-regulates CD133 expression in CD133-overexpressing gastrointestinal cancer cells. We examined the mRNA expression levels of CD133 in 26 cancer cell

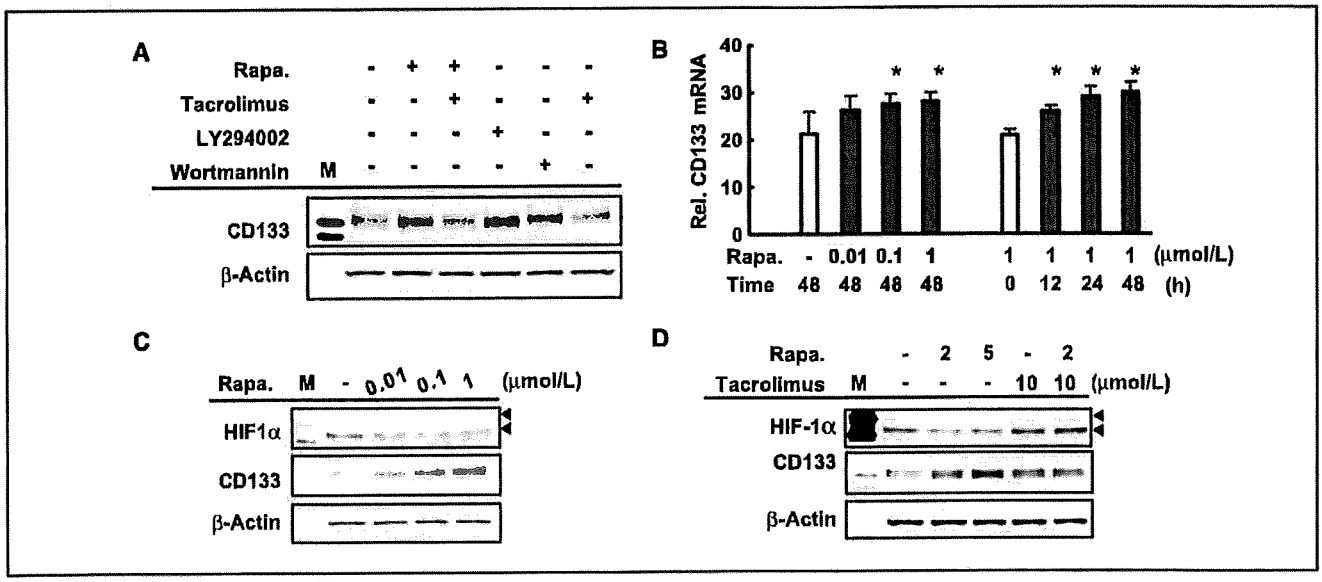

Figure 2. Rapamycin down-regulates HIF-1α expression and up-regulates CD133 expression at the transcriptional level. *A*, WiDr cells were exposed to rapamycin, the rapamycin-competitor tacrolimus, and the phosphoinositide-3-kinase inhibitors LY294002 and wortmannin for 48 h at concentrations of 10 μmol/L. The inhibition of mTOR signaling up-regulated CD133 expression. *B*, rapamycin up-regulated the expression of CD133 mRNA in WiDr cells in a time-dependent and dose-dependent manner. *Columns*, mean determined using real-time RT-PCR; *bars*, SD. *C* and *D*, rapamycin exposure and HIF-1α expression. WiDr cells were exposed to rapamycin with/without tacrolimus at the indicated concentration for 48 h. Rapamycin down-regulated HIF-1α expression and inversely up-regulated CD133 expression; these effects were canceled by tacrolimus. *Rel. CD133 mRNA*, normalized mRNA expression levels (CD133/GAPD × 10^4); *Rapa.*, rapamycin.

lines using real-time RT-PCR. Several gastric, colorectal, and lung cancer cell lines such as SNU16, IM95, HSC43, WiDr, and H69, overexpressed CD133 (Fig. 1*A*). The increased expression of CD133 protein was also confirmed in these cell lines (Fig. 1*B*). The mTOR inhibitor rapamycin, but not cytotoxic drugs (5-fluorouracil, CPT-11, and gemcitabine), increased the expression of CD133 in a dose-dependent manner in CD133-overexpressing WiDr cells (Fig. 1*C* and *D*). These results indicate that mTOR signaling is involved in the expression of CD133 in cancer cells.

Rapamycin down-regulated HIF-1α expression and up-regulated CD133 expression at the transcriptional level. To examine the signal transduction of rapamycin-induced CD133 expression, we used the rapamycin-competitor tacrolimus and the phosphoinositide-3-kinase inhibitors LY294002 and wortmannin. Tacrolimus (10 μmol/L) completely canceled the up-regulation of CD133 induced by rapamycin. The inhibition of phosphoinositide-3-kinase by LY294002 (10 μmol/L) and wortmannin (10 μmol/L) also up-regulated CD133 expression (Fig. 2*A*). Rapamycin up-regulated CD133 expression at the transcriptional level in a dose-dependent and time-dependent manner (Fig. 2*B*).

The inhibition of mTOR signaling is likely to lead to the down-regulation of the expression of certain molecules because the mTOR complex positively regulates the general translational machinery. Under the inhibition of mTOR signaling, HIF-1α, among several downstream molecules of mTOR, can activate transcription by acting as a repressor of specific transcription factors such as the MYC-associated protein X homodimer (11). Therefore, we focused on the possible role of HIF-1α in the regulation of CD133 expression. Rapamycin down-regulated HIF-1α expression but up-regulated CD133 expression (Fig. 2*C*). Meanwhile, tacrolimus canceled the effect of rapamycin on the expressions of HIF-1α and CD133 (Fig. 2*D*). These results suggest that the down-regulation of HIF-1α may mediate the up-regulation of CD133 expression in cancer cells. Up-regulation of CD133 expression by rapamycin was reproducibly observed in the CD133 high-expressing cell lines, but not in CD133 low-expressing cell lines (Supplemental Fig. S2).

Induction of HIF-1α down-regulates CD133 expression in cancer cells. Hypoxia mediates the stabilization of HIF-1α protein and enables its escape from rapid degradation, facilitating the up-regulation of HIF-1α expression (12). Hypoxia strongly induced HIF-1α expression, whereas CD133 expression was down-regulated in all three CD133-overexpressing cell lines (Fig. 3*A*). Rapamycin dose-dependently up-regulated CD133 expression under normoxic conditions, but no effect was seen under hypoxic conditions. We speculated that the effect of hypoxia on the induction of HIF-1α is much higher than the effect of rapamycin on the down-regulation of HIF-1α. The expression of CD133 mRNA was also strongly down-regulated under hypoxic conditions in all three cell lines (Fig. 3*B*) and in three additional cell lines (Supplemental Fig. S1).

In addition, DFO, a known HIF-1α activator, induced HIF-1α expression in a dose-dependent manner but down-regulated the expression of CD133 at both the mRNA and protein levels in WiDr cells (Fig. 3*C* and *D*), and in three additional cell lines (Supplemental Fig. S2). These results were consistent with those obtained under hypoxic conditions. Both hypoxia and DFO exposure markedly down-regulated CD133 expression, strongly suggesting that induction of HIF-1α results in the down-regulation of CD133 expression.

Inverse correlation between CD133 and HIF-1α in clinical samples. Finally, to address whether CD133 and HIF-1α expression are inversely correlated in clinical samples of gastric cancer

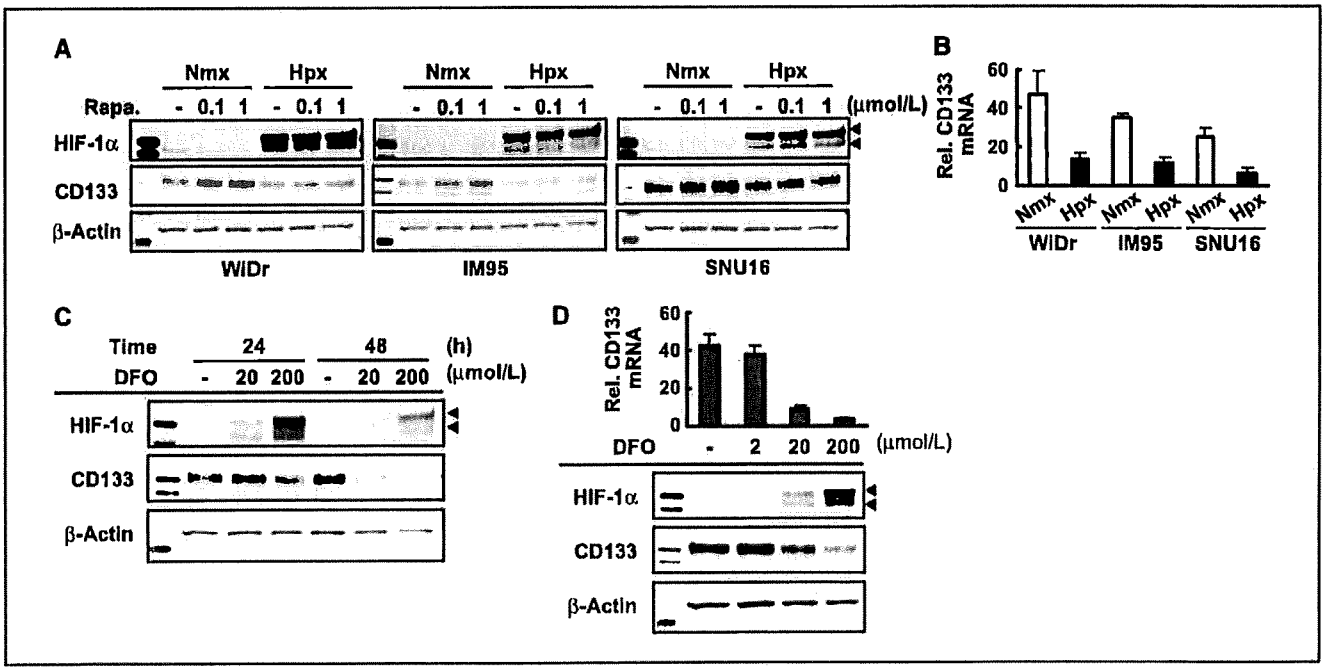

Figure 3. Induction of HIF-1α down-regulates CD133 expression in cancer cells. *A*, three gastrointestinal cancer cell lines were exposed to rapamycin under normoxic or hypoxic conditions for 24 h. Hypoxia induced HIF-1α expression and inversely down-regulated CD133 expression. *B*, hypoxia strongly down-regulated CD133 expression at the mRNA level. *Columns*, mean determined using real-time RT-PCR; *bars*, SD. *C*, DFO, a known HIF-1α activator, induced HIF-1α expression and down-regulated CD133 expression in WiDr cells. *D*, DFO induced these effects at both the mRNA and protein levels. Note that both hypoxia and DFO exposure had similar effects on HIF-1α induction and CD133 down-regulation. *Rel. CD133 mRNA*, normalized mRNA expression levels (CD133/GAPD × 10^4); *Rapa.*, rapamycin.

specimens, we examined the expression of these molecules using previously published microarray data (9). The expressions of CD133 and HIF-1α were inversely correlated in gastric cancer ($r = -0.68$; Fig. 4*A*), whereas the expressions of CD133 and HIF-1β were not ($r = -0.05$; Fig. 4*A*). These results are consistent with the *in vitro* findings in the present study.

Taken together, the present results suggest that an oxygen-sensitive intracellular pathway involving both HIF-1α and mTOR signaling may, at least in part, regulate CD133 expression in cancer cells (shown in the schema in Fig. 4*B*).

Discussion

Hypoxic conditions promote the proliferation of mammalian ES cells more efficiently than normoxia and are thought to be required for the maintenance of full pluripotency. Hematopoietic stem cells are located in the bone marrow, which is a physiologically hypoxic environment, and the survival and/or self-renewal of hematopoietic stem cells is enhanced *in vitro* if the cells are cultured under hypoxic conditions (13). Thus, accumulating data indicates that oxygen levels influence specific cell fates in several developmental processes; however, the effect of oxygen levels on cell differentiation is thought to be context-dependent (14). Our data on CD133 expression in response to hypoxia were different from the previous study shown in glioma (5). The discrepancy might be explained by (*a*) a different cellular context in glioma from the others, because CD133 expressions of all cell lines including the WiDr, IM95, SNU16, OCUM1, 44As3, and DLD-1 cells were reproducibly down-regulated by hypoxic condition (Supplemental Fig. S1; Fig. 3*B*), whereas the U251 cells failed to exhibit the down-regulation, and by (*b*) the different detection methods in our study (Western blot and quantitative real-time RT-PCR) from the previous report (flow cytometry for CD133-positive cells).

The detailed mechanism responsible for the repressive role of HIF-1α on CD133 expression is not fully understood; one possible explanation is raised by MYC, which is also known as c-Myc. HIF-1α binds to MAX and renders MYC inactive, and HIF-1 (homodimers of HIF-1α and HIF-1β) activates the expression of MXI1 (MAX interactor 1), which binds to MAX and thereby antagonizes MYC function (11). Recent reports have shown that HIF-1α inhibits MYC activity, which is thought to have implications for stem cell function (15, 16). Whether MYC directly activates CD133 transcription remains unclear; our preliminary data indicate that a MYC-inhibitor suppressed CD133 expression in WiDr cells.[4] Because the gene amplification of MYC and MYCN is frequently observed in many cancers, the relations among MYC, HIF-1α, HIF-1β, HIF-2, and CD133 should be investigated in future studies.

In conclusion, we showed that the inhibition of mTOR signaling up-regulated CD133 expression, whereas HIF-1α induction under hypoxic conditions or DFO exposure down-regulated CD133 expression in gastrointestinal cancer cells. Our findings show a novel regulatory mechanism for the expression of CD133 involving mTOR signaling and HIF-1α, and these findings may contribute to our understanding of the stemness character of cancer stem cells.

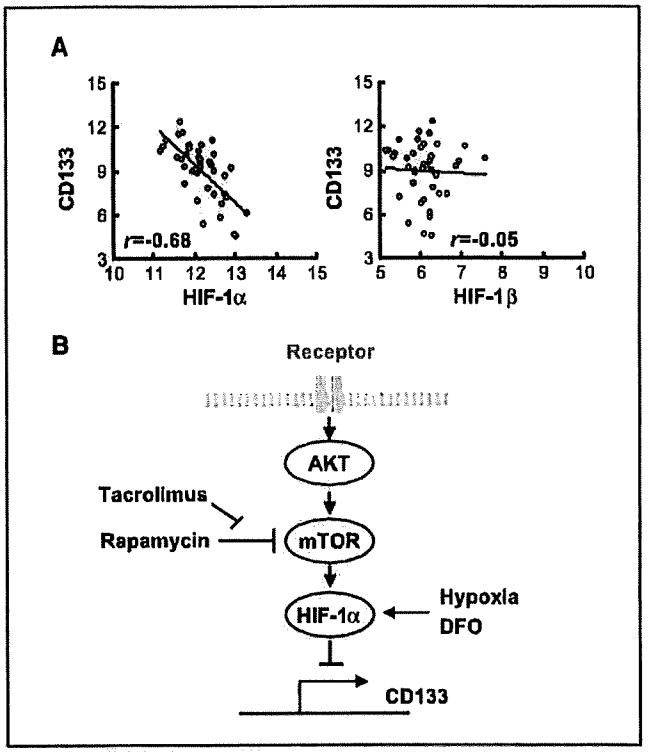

Figure 4. Inverse correlation between CD133 and HIF-1α in clinical samples of gastric cancer. *A*, the correlation between the expressions of CD133 and HIF-1α were analyzed in 40 clinical gastric cancer specimens using previously published microarray data. CD133 and HIF-1α were inversely correlated in gastric cancer ($r = -0.68$), whereas CD133 and HIF-1β were not ($r = -0.05$). *B*, proposed model depicting the involvement of mTOR signaling, HIF-1α, and CD133 expression. HIF-1α, a downstream molecule of mTOR, down-regulates CD133 expression at the transcriptional level in cancer cells.

Disclosure of Potential Conflicts of Interest

No potential conflicts of interest were disclosed.

Acknowledgments

Received 4/7/09; revised 6/2/09; accepted 6/30/09; published OnlineFirst 9/8/09.

Grant support: 3rd Term Comprehensive 10-Year Strategy for Cancer Control, the program for the promotion of Fundamental Studies in Health Sciences of the National Institute of Biomedical Innovation, and a Grant-in-aid for Scientific Research from the Ministry of Education, Culture, Sports, Science and Technology of Japan (19790240 and 19209018).

The costs of publication of this article were defrayed in part by the payment of page charges. This article must therefore be hereby marked *advertisement* in accordance with 18 U.S.C. Section 1734 solely to indicate this fact.

[4] Unpublished data.

References

1. Neuzil J, Stantic M, Zobalova R, et al. Tumour-initiating cells vs. cancer "stem" cells and CD133: what's in the name? Biochem Biophys Res Commun 2007;355:855–9.
2. Fan X, Matsui W, Khaki L, et al. Notch pathway inhibition depletes stem-like cells and blocks engraftment in embryonal brain tumors. Cancer Res 2006;66:7445–52.
3. Clement V, Sanchez P, de Tribolet N, Radovanovic I, Ruiz i Altaba A. HEDGEHOG-GLI1 signaling regulates human glioma growth, cancer stem cell self-renewal, and tumorigenicity. Curr Biol 2007;17:165–72.
4. Piccirillo SG, Reynolds BA, Zanetti N, et al. Bone morphogenetic proteins inhibit the tumorigenic potential of human brain tumour-initiating cells. Nature 2006;444:761–5.

5. Platet N, Liu SY, Atifi ME, et al. Influence of oxygen tension on CD133 phenotype in human glioma cell cultures. Cancer Lett 2007;258:286–90.
6. Chen HL, Pistollato F, Hoeppner DJ, Ni HT, McKay RD, Panchision DM. Oxygen tension regulates survival and fate of mouse central nervous system precursors at multiple levels. Stem Cells 2007;25:2291–301.
7. Hudson CC, Liu M, Chiang GG, et al. Regulation of hypoxia-inducible factor 1α expression and function by the mammalian target of rapamycin. Mol Cell Biol 2002; 22:7004–14.
8. Chiang GG, Abraham RT. Targeting the mTOR signaling network in cancer. Trends Mol Med 2007;13: 433–42.
9. Yamada Y, Arao T, Gotoda T, et al. Identification of prognostic biomarkers in gastric cancer using endoscopic biopsy samples. Cancer Sci 2008;99: 2193–9.
10. Takeda M, Arao T, Yokote H, et al. AZD2171 shows potent antitumor activity against gastric cancer over-expressing FGFR2/KGFR. Clin Cancer Res 2007;13: 3051–7.
11. Dang CV, Kim JW, Gao P, Yustein J. The interplay between MYC and HIF in cancer. Nat Rev Cancer 2008;8: 51–6.
12. Wouters BG, Koritzinsky M. Hypoxia signalling through mTOR and the unfolded protein response in cancer. Nat Rev Cancer 2008;8:851–64.
13. Danet GH, Pan Y, Luongo JL, Bonnet DA, Simon MC. Expansion of human SCID-repopulating cells under hypoxic conditions. J Clin Invest 2003;112:126–35.
14. Simon MC, Keith B. The role of oxygen availability in embryonic development and stem cell function. Nat Rev Mol Cell Biol 2008;9:285–96.
15. Koshiji M, Kageyama Y, Pete EA, Horikawa I, Barrett JC, Huang LE. HIF-1α induces cell cycle arrest by functionally counteracting Myc. EMBO J 2004;23: 1949–56.
16. Zhang H, Gao P, Fukuda R, et al. HIF-1 inhibits mitochondrial biogenesis and cellular respiration in VHL-deficient renal cell carcinoma by repression of C-MYC activity. Cancer Cell 2007;11:407–20.